Laboratory
Underground
Nuclear
Astrophysics

Recent results and status of the $^{14}N(p,\gamma)^{15}O$ measurement at LUNA

Heide Costantini
Dipartimento di Fisica and INFN, Genova (Italy)

Laboratory for Underground Nuclear Astrophysics

Gran Sasso National Laboratory (LNGS)

Cosmic background reduction: μ: 10^{-6} n: 10^{-3}

50 KV : (1992-2001)

- $^{3}He(^{3}He,2p)^{4}He$
- $d(^{3}He,p)^{4}He$
- $d(p,\gamma)^{3}He$

400 KV: (2000→...)

$^{14}N(p,\gamma)^{15}O$ (CNO cycle)

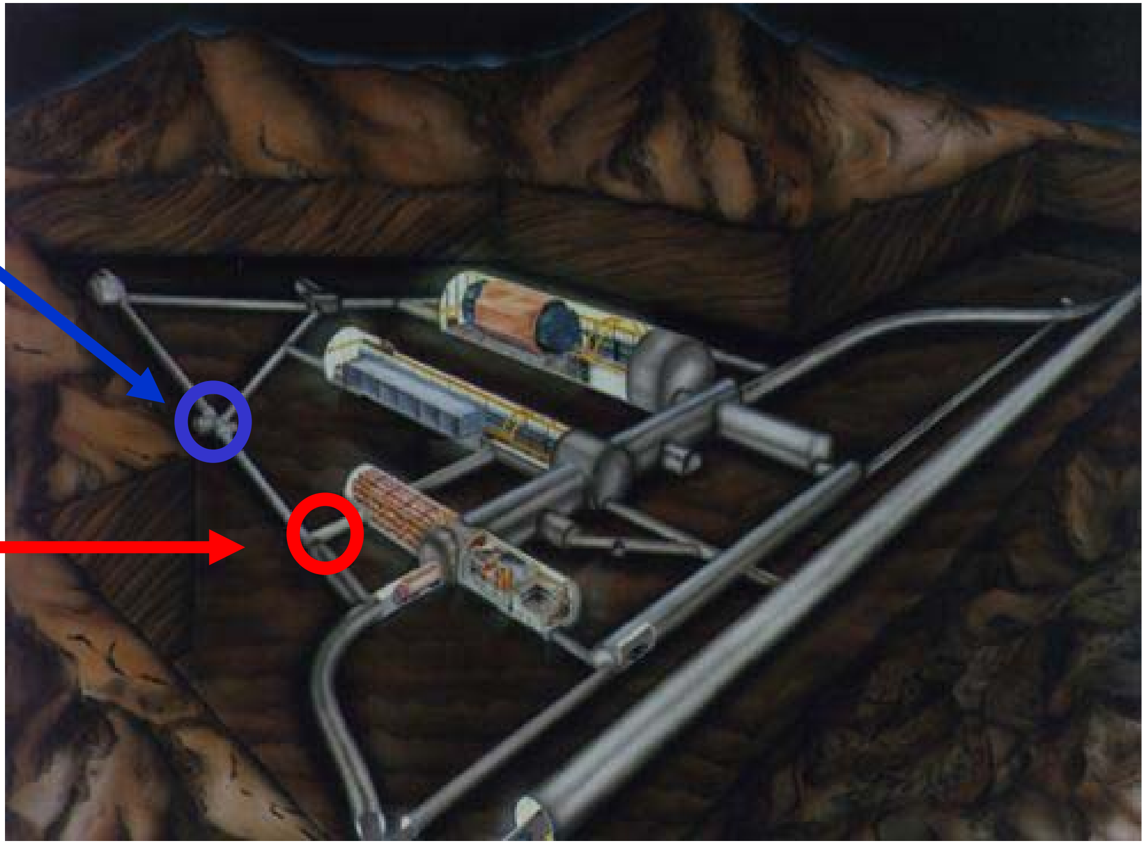

400 kV accelerator

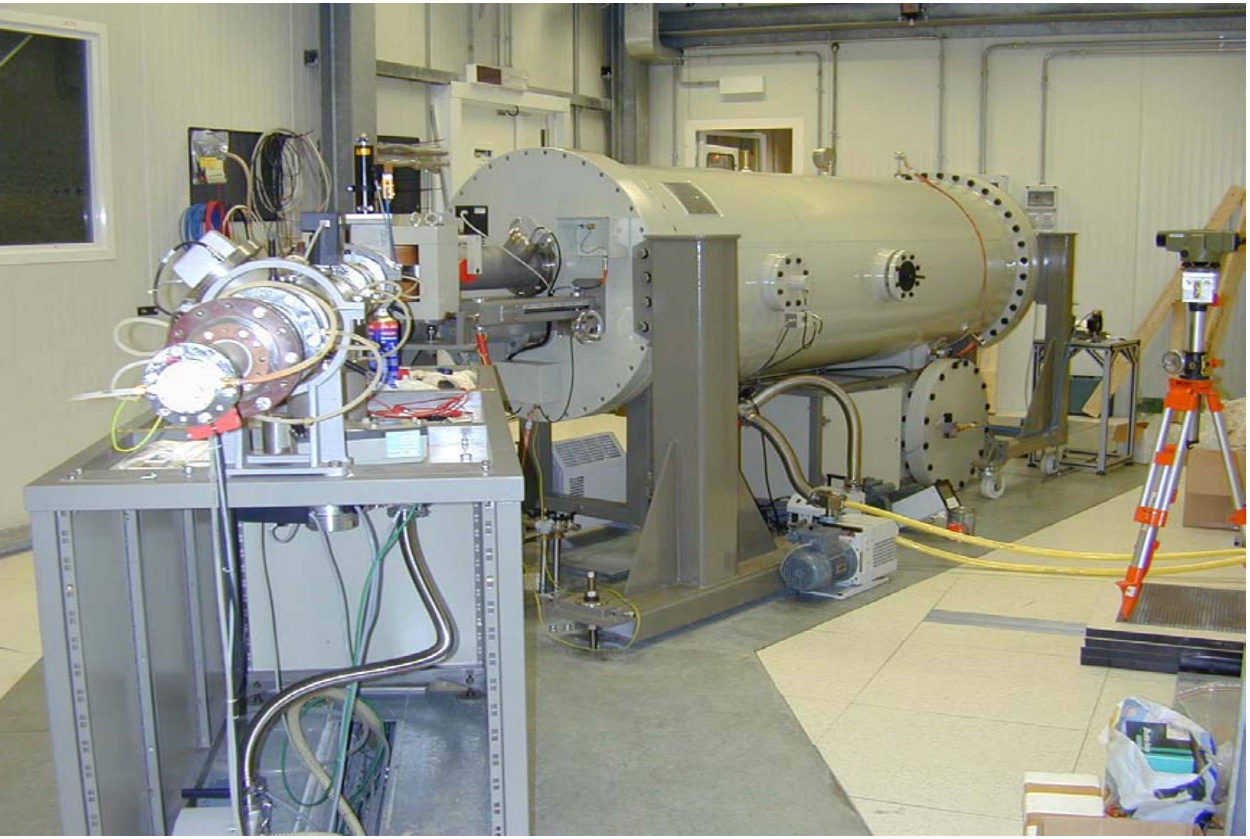

SPECIFICATIONS

- ✓ U_{max}= 50 - 400 kV
- ✓ $I \sim 500\ \mu A$ for protons
- ✓ DE_{max}= 0.07 keV

- Energy spread : 72eV
- Total uncertainty is ±300 eV between Ep=100 ÷ 400keV

Present and future activity:

- ☞ $^{14}N(p,\gamma)^{15}O$ in progress...
- ☞ $^{4}He(^{3}He,\gamma)^{7}Be$
- ☞ $^{25}Mg(p,\gamma)^{26}Al$

$^{14}N(p,\gamma)^{15}O$ and solar neutrinos

- The rate of the CNO cycle is governed by the slowest reaction $^{14}N(p,\gamma)^{15}O$ (Q=7.3 MeV)

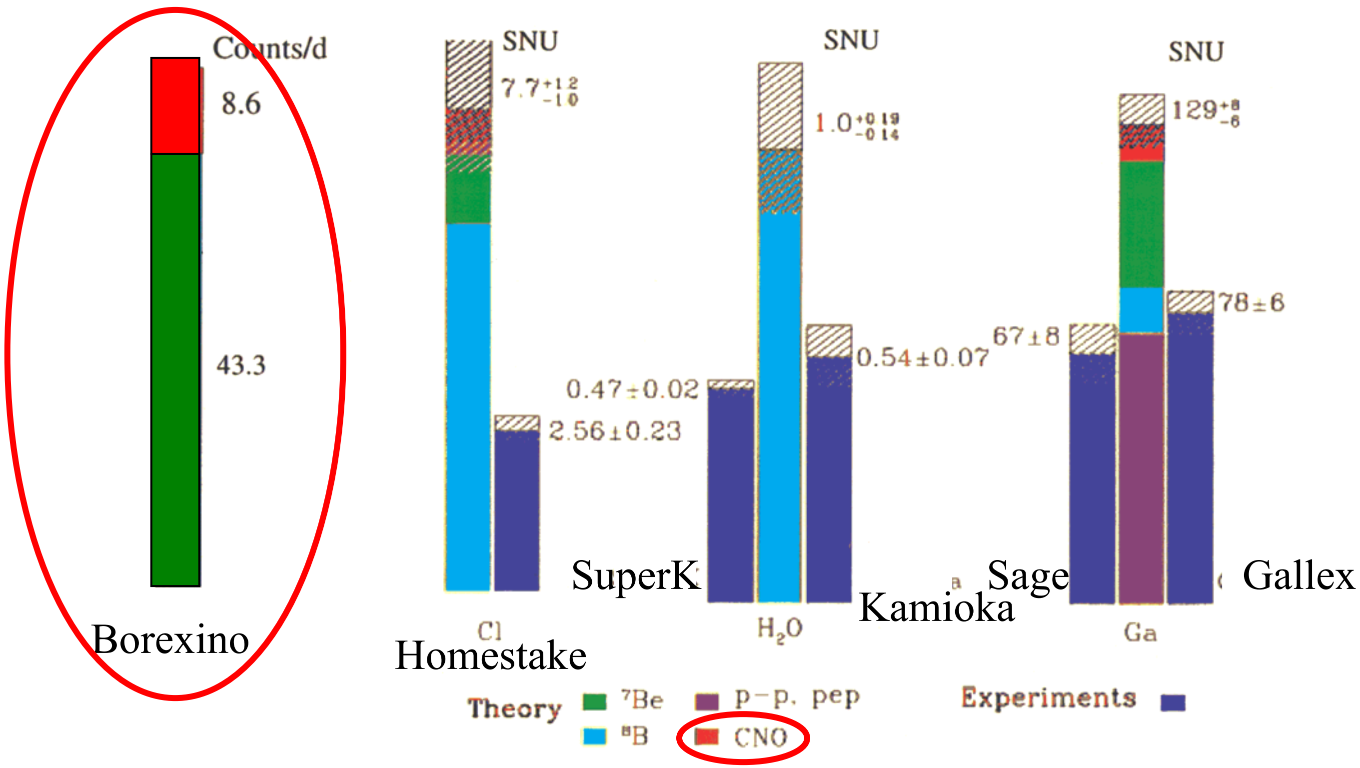

- ^{13}N and ^{15}O neutrinos have fluxes and energy spectra comparable with those coming from ^7Be (pp chain)

Globular Clusters and $^{14}N(p,\gamma)^{15}O$ reaction rate

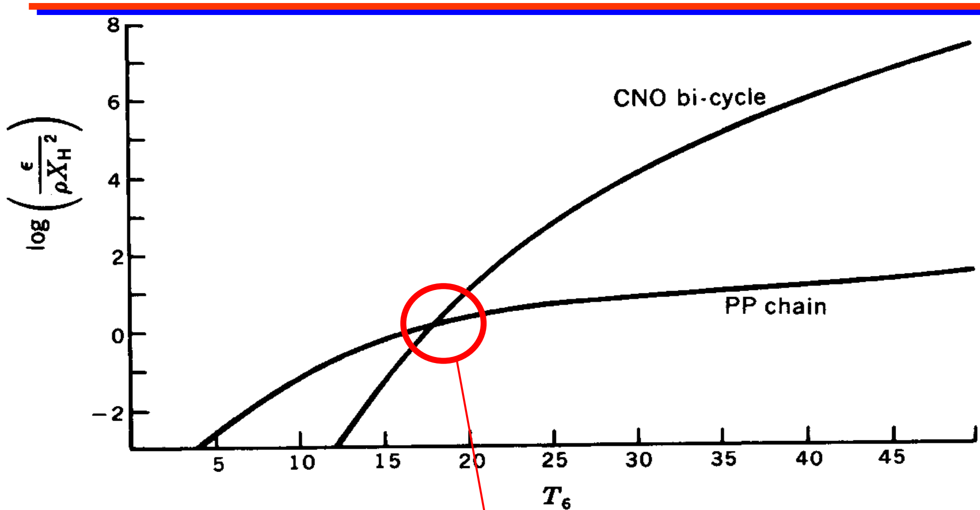

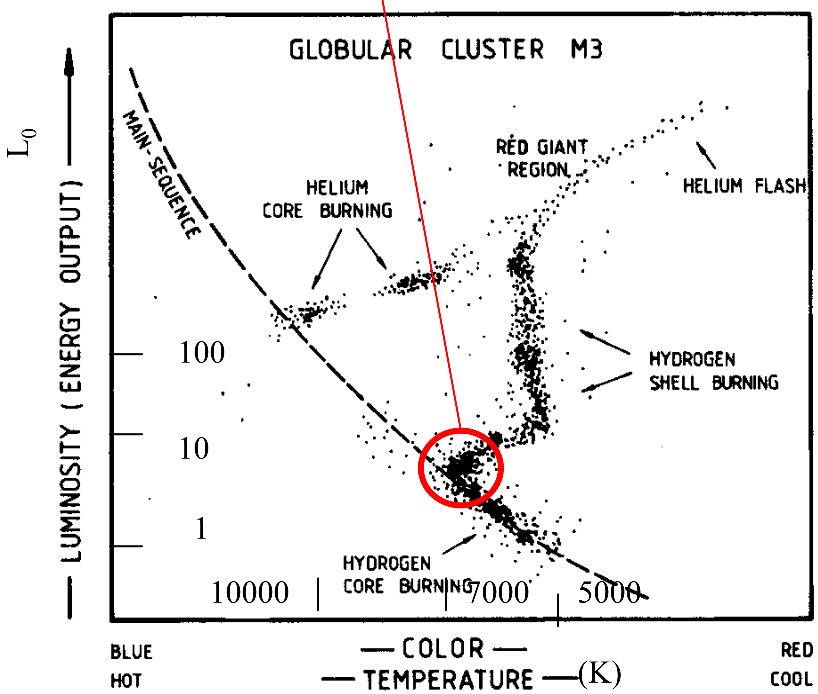

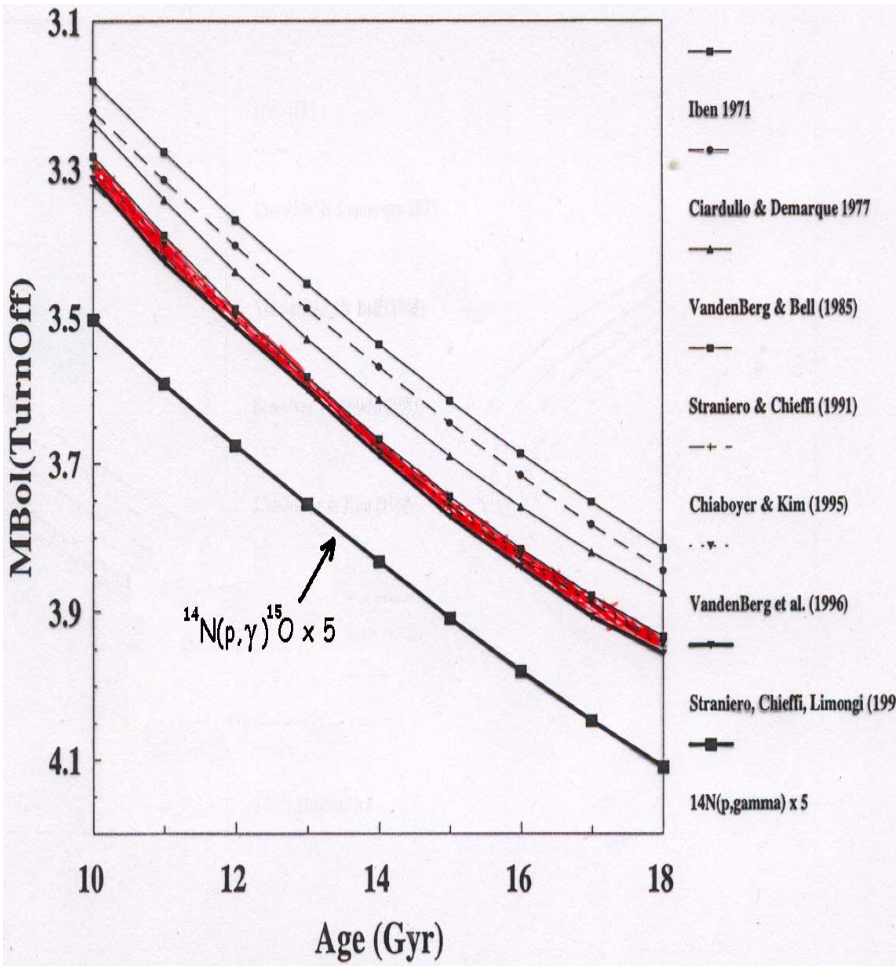

$^{14}N(p,\gamma)^{15}O$

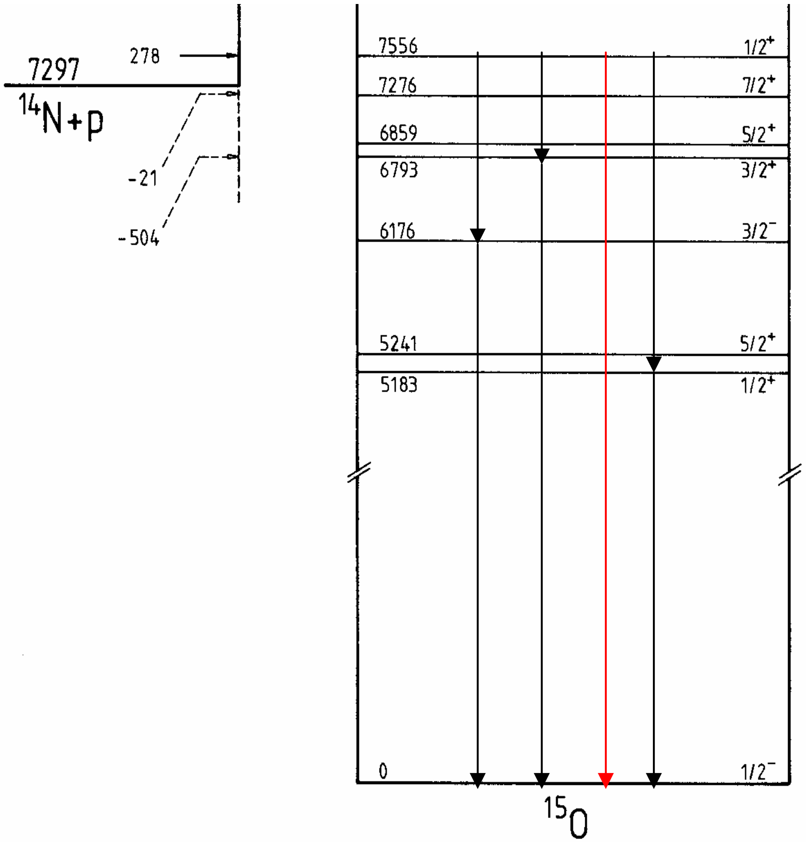

Schröder et al. (1987)
Nucl. Phys A

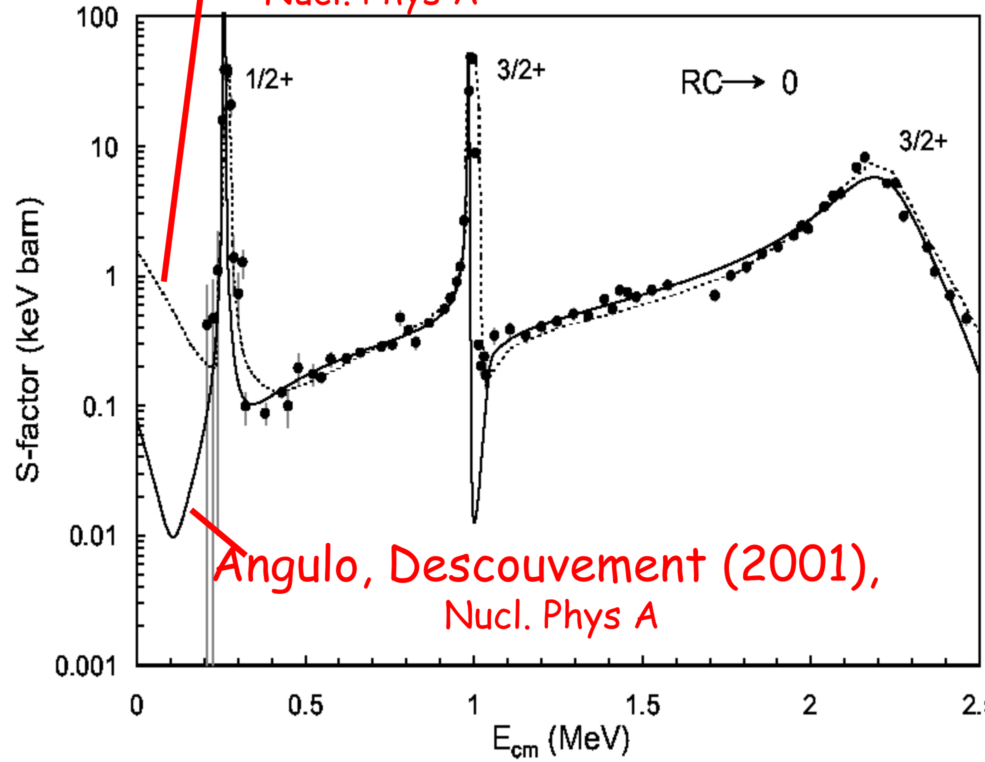

Angulo, Descouvement (2001),
Nucl. Phys A

R/DC → 0

S(0) = 1.55 ± 0.34 keV-b (Schröder)

S(0) = 0.08 ±0.06 keV-b (Angulo)

2 experimental approaches

Gas target + BGO summing crystal

- Pure target
- Stable target

- total-S(E)
- Low resolution
- High efficiency

$E_{min} < 100$ keV

Solid target + HpGe detector

- angular distribution
- high density

- Single γ transitions
- Low efficiency
- High resolution

$E_{min} \approx 140$ keV

Experimental setup

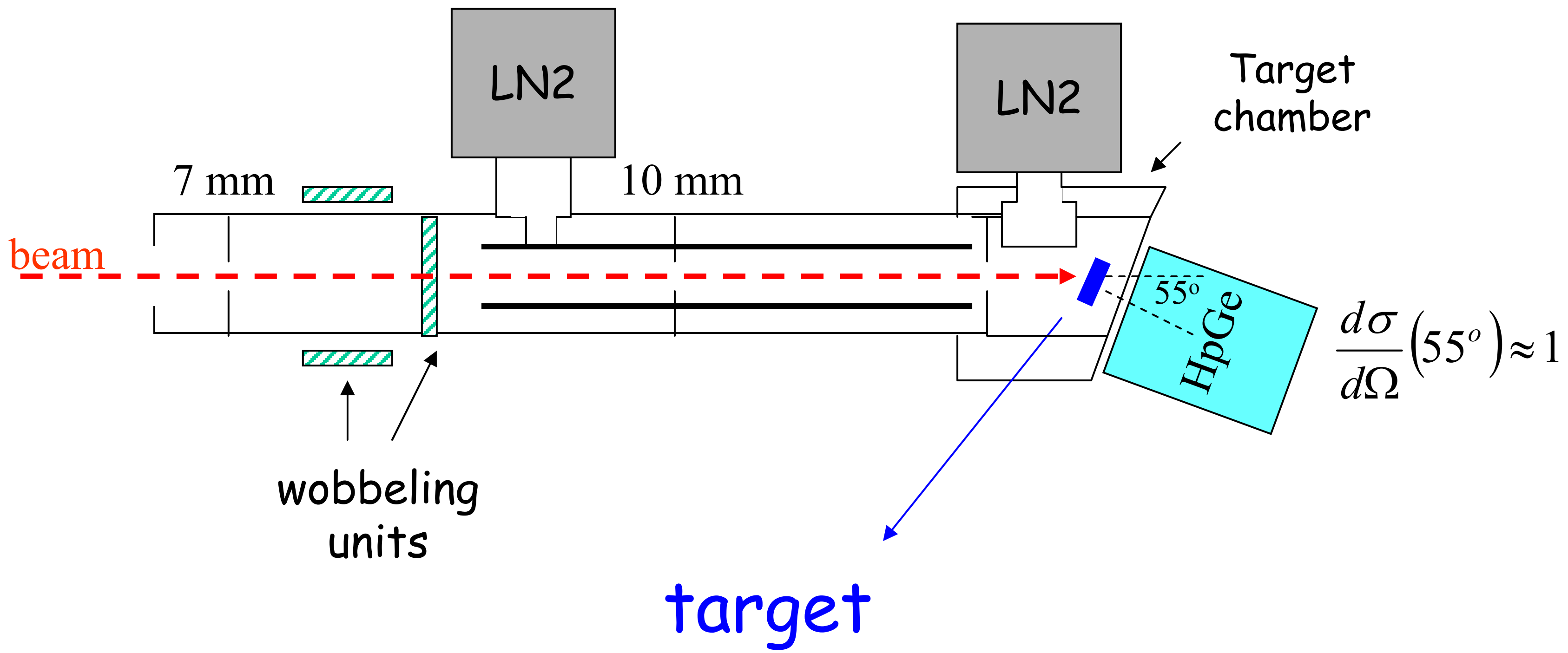

High density

High stability

High purity

→

TiN deposited on Ta

Solid Target features

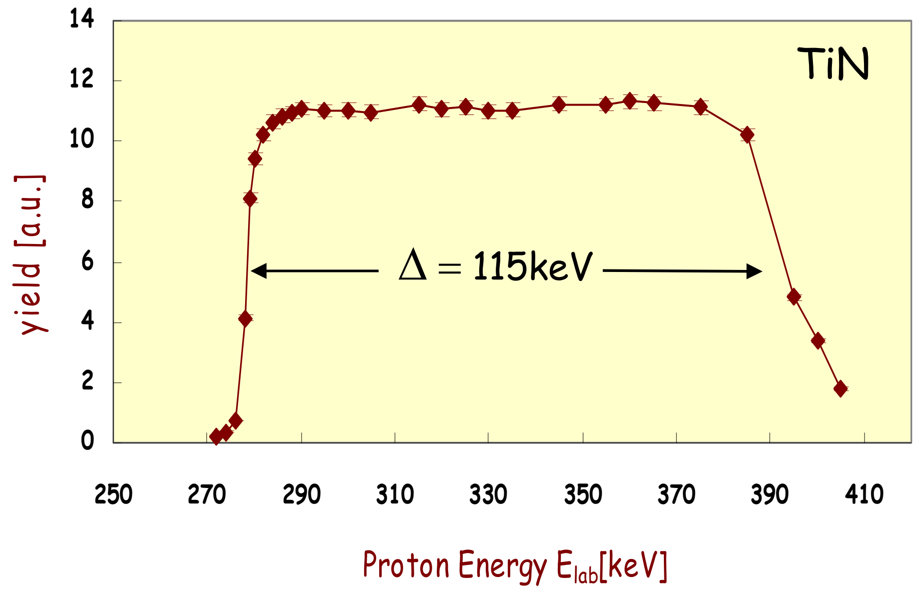

$^{14}N(p,\gamma)^{15}O$ E_R=278 keV

Target profile
(thickness, homogeneity)

Target stability

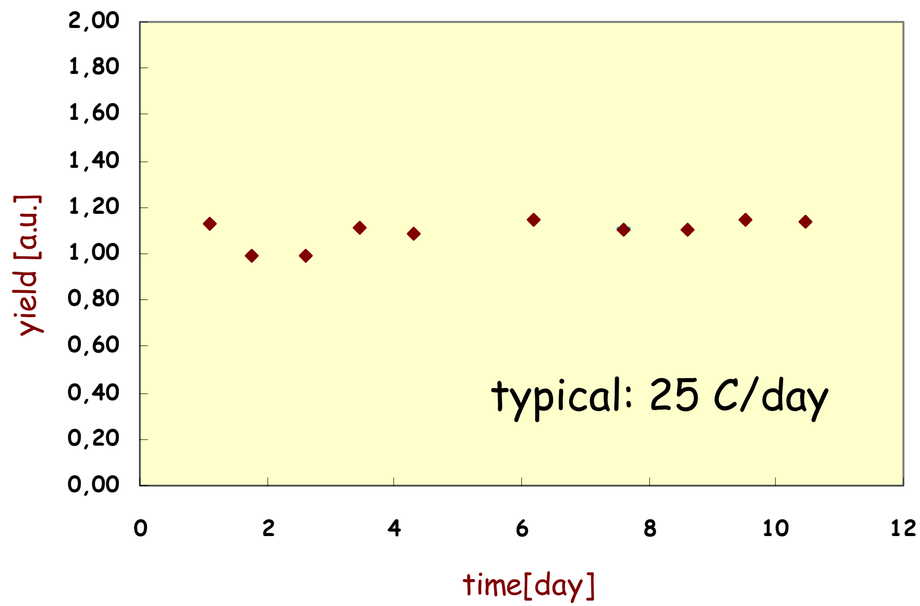

HpGe background

At surface

3MeV < Eγ < 8MeV

0.5 Counts/s

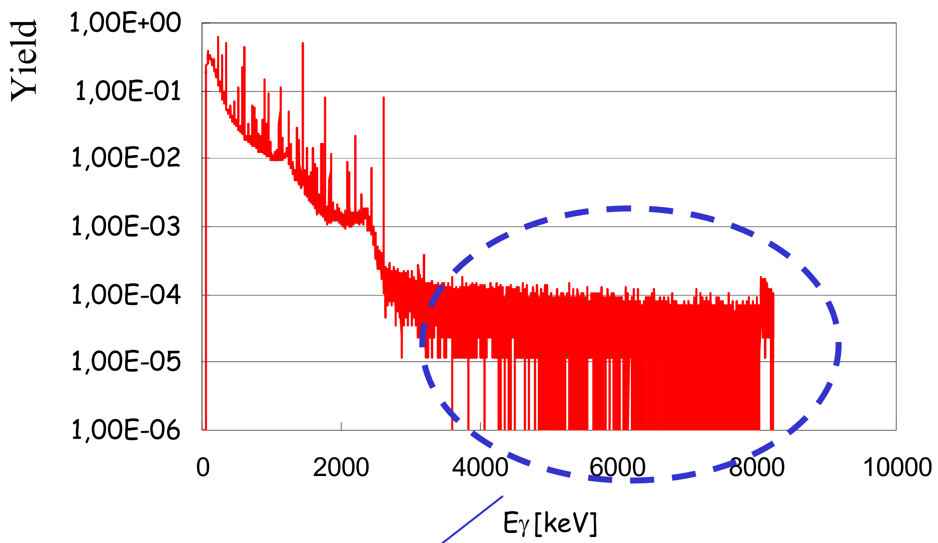

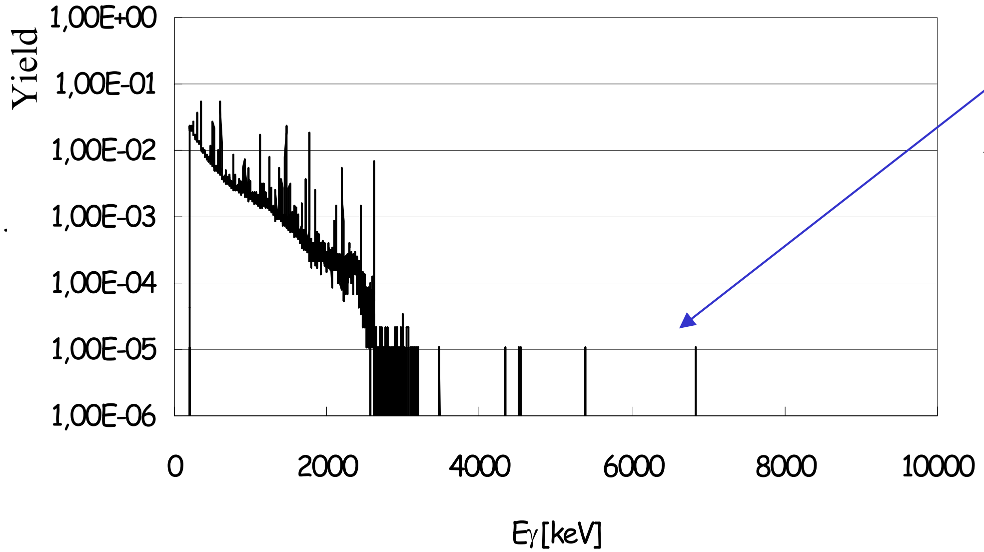

Underground

3MeV < Eγ < 8MeV

0.0002 Counts/s

Beam induced background

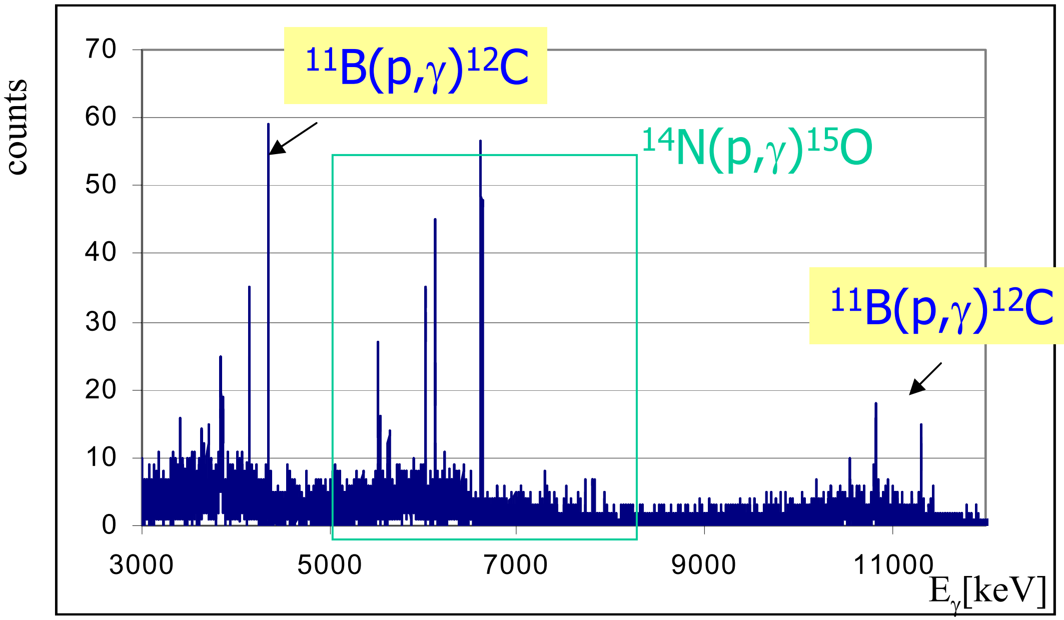

E_{beam}= 200 keV

E_{beam}= 140 keV

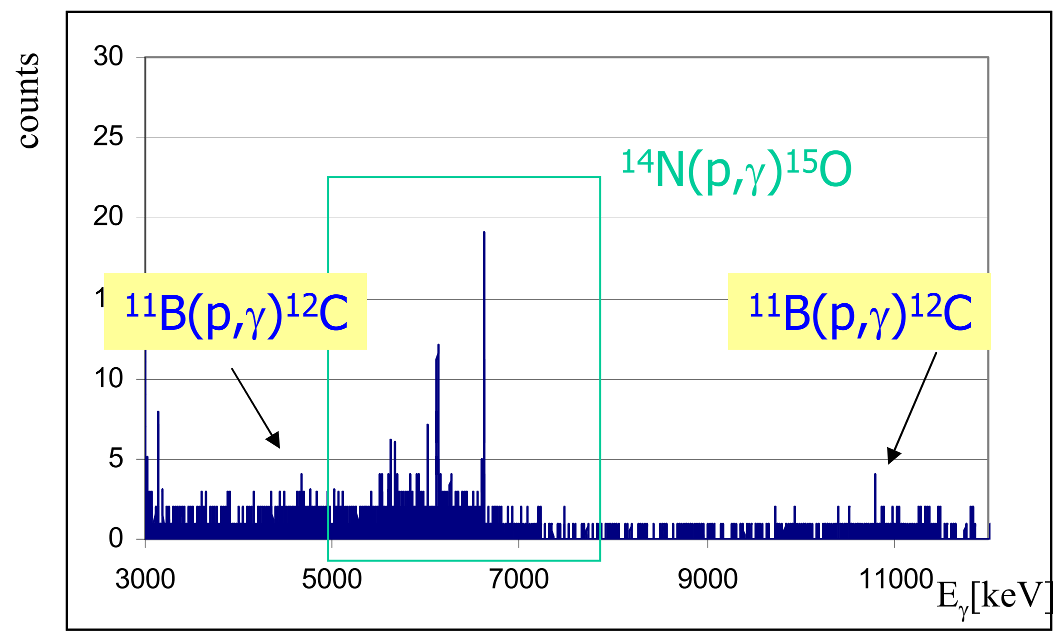

The experimental spectrum

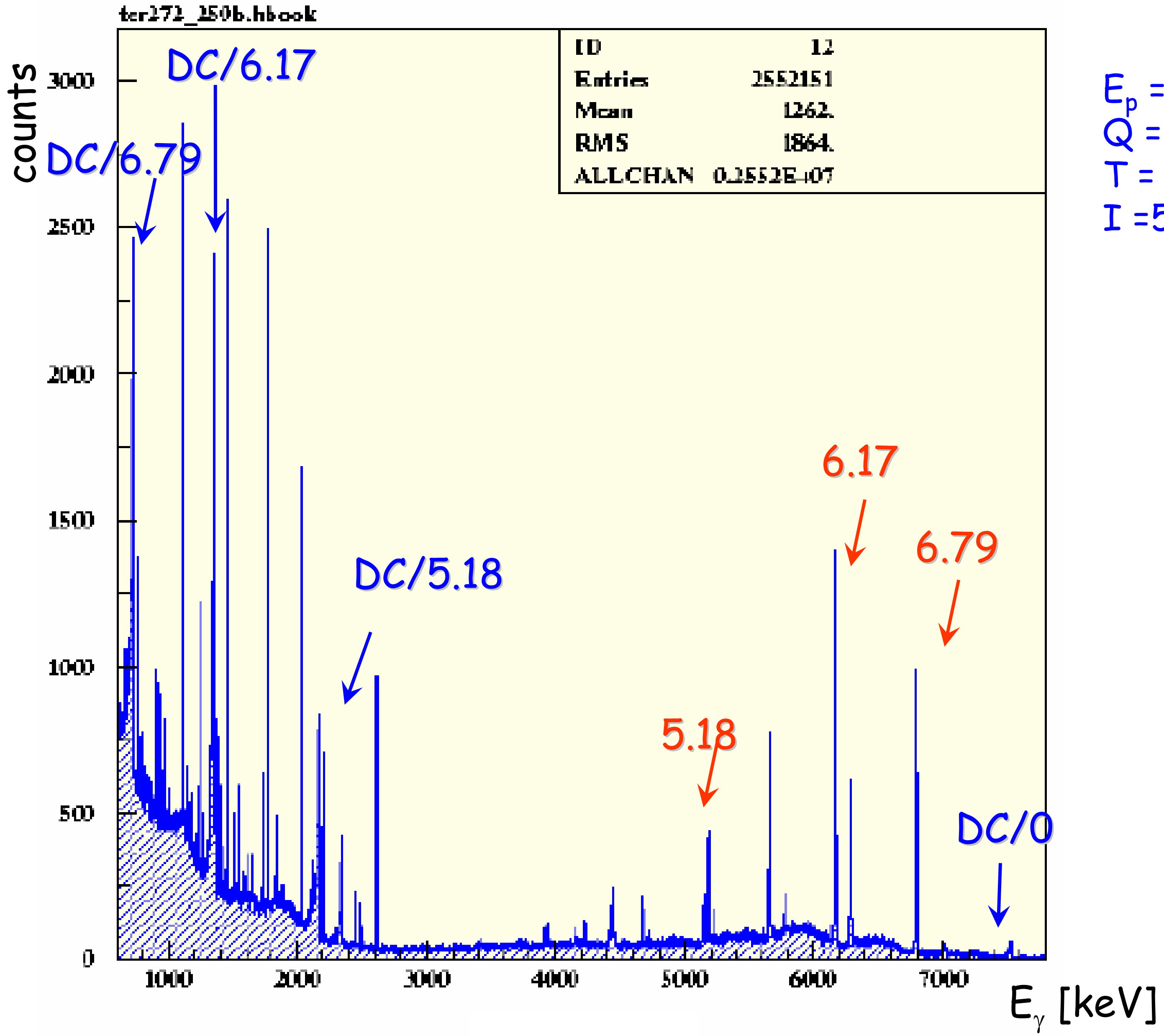

E_p = 250 keV
Q = 41.2 C
T = 20 h
I = 570 μA

Summing effect

In close geometry meas. high summing effect probability

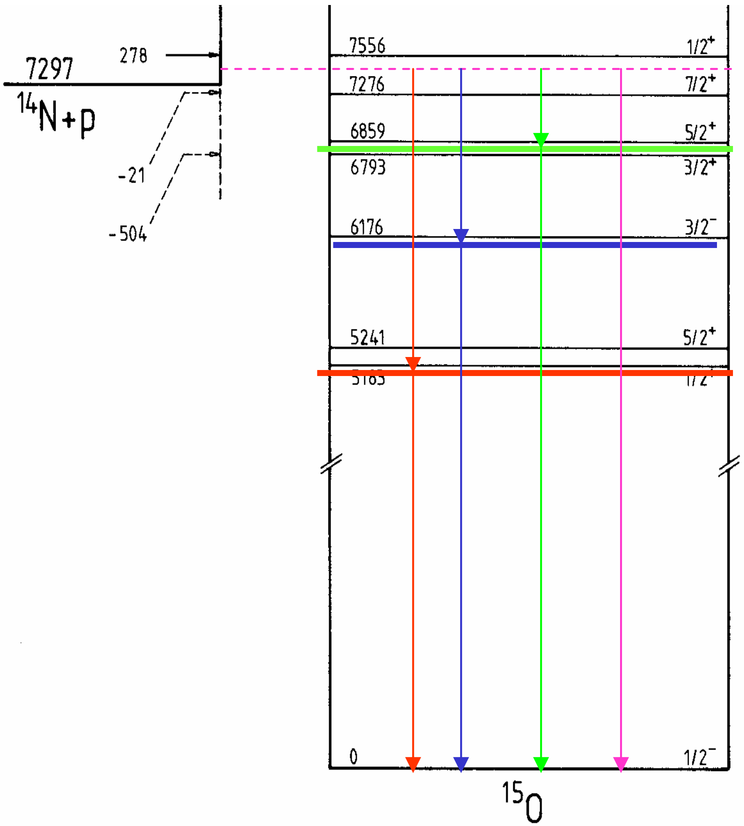

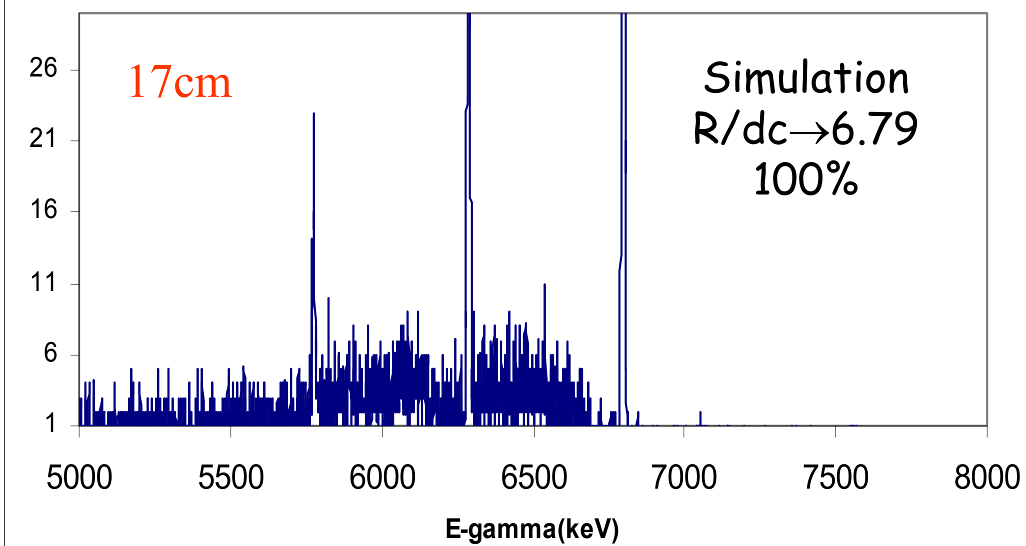

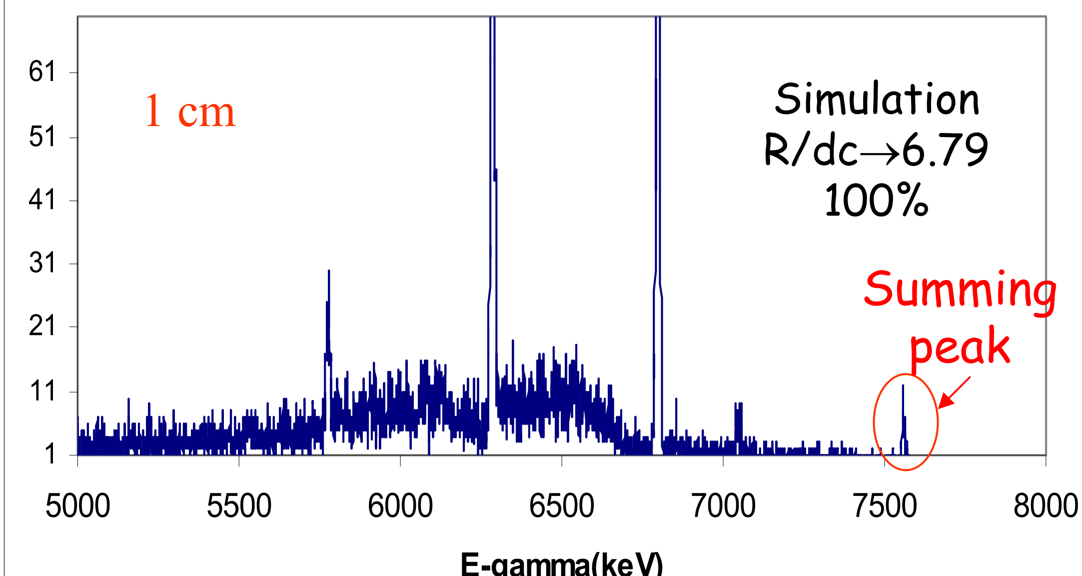

278 keV resonance parameters

- Resonance strength

present work	literature
$(13.5 \pm 0.4 \pm 0.8)$ meV	(14 ± 2) meV

- Branching ratios at the 278 keV resonance

	present work	literature
R/DC→0	1.7±0.1	3.5 ±0.5
R/DC→6.79	23.3 ±0.3	23.3 ±0.6
R/DC→6.17	58.4 ±0.3	57.4 ±0.6
R/DC→5.18	16.6 ±0.2	17.1 ±0.6

← Hebbard & Bailey (1963)

Close geometry measurements → Summing effect

Angular distribution measurements

beam

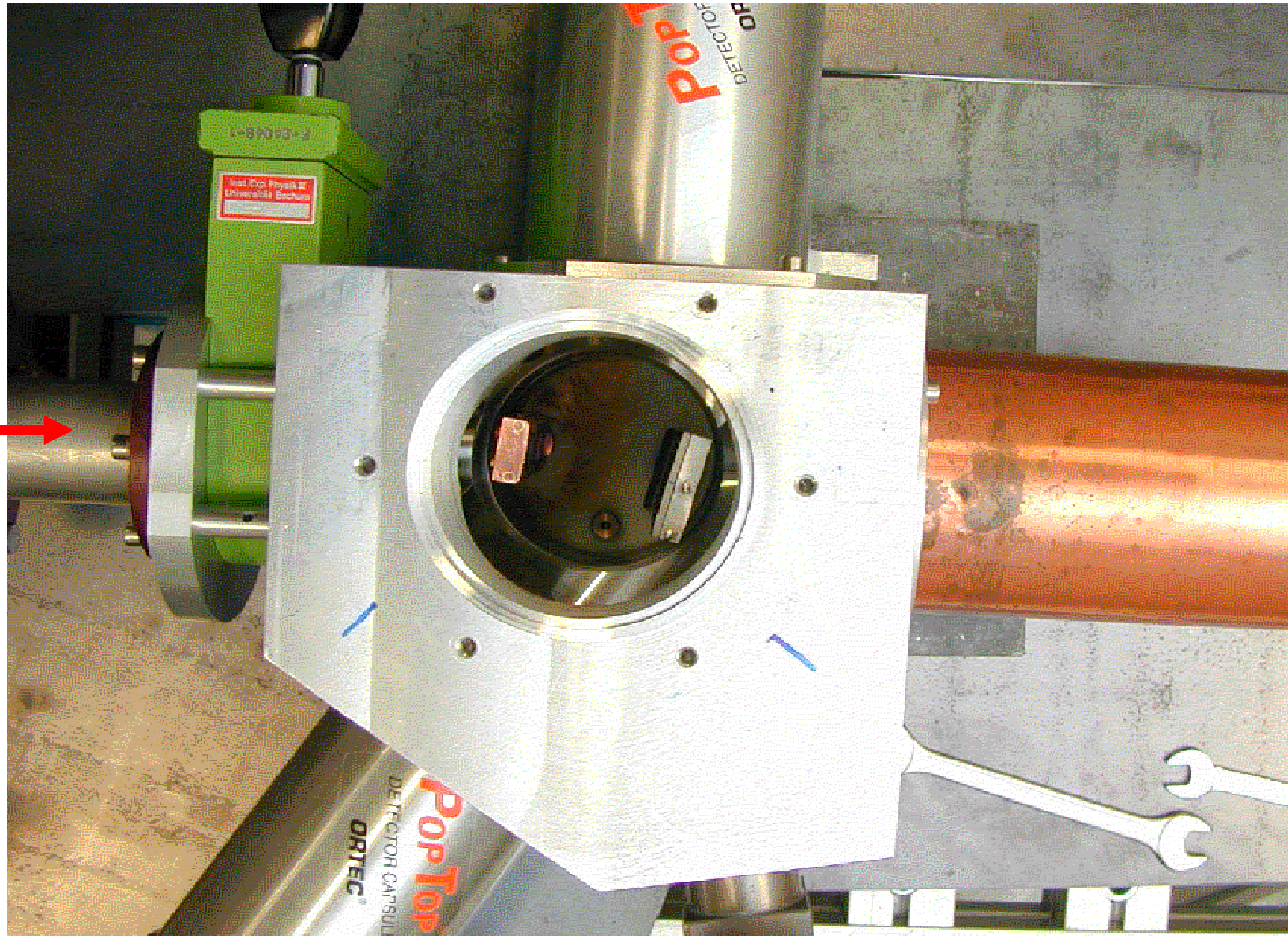

E_{lab} = 220 keV

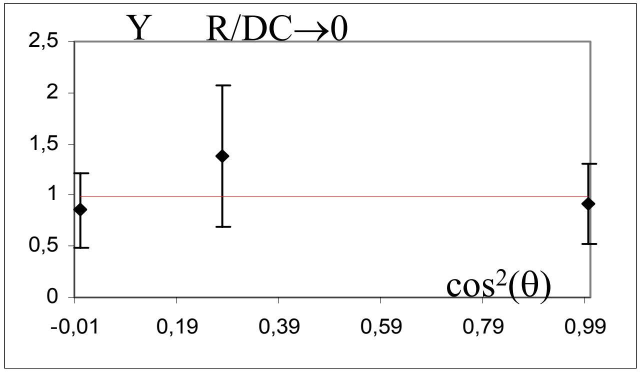

$$\frac{d\sigma}{d\Omega} = 1 + a_1 P_1(\vartheta) + a_2 P_2(\vartheta) + \ldots$$

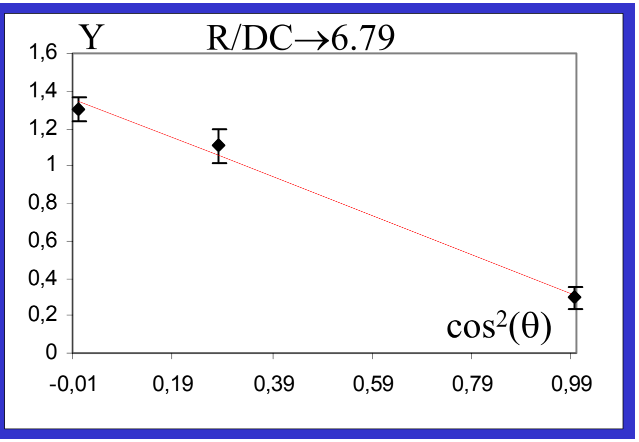

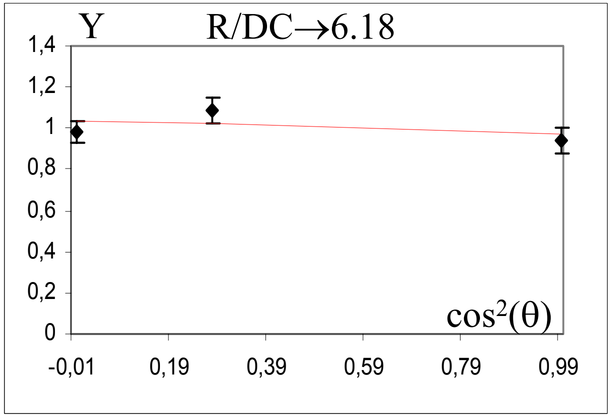

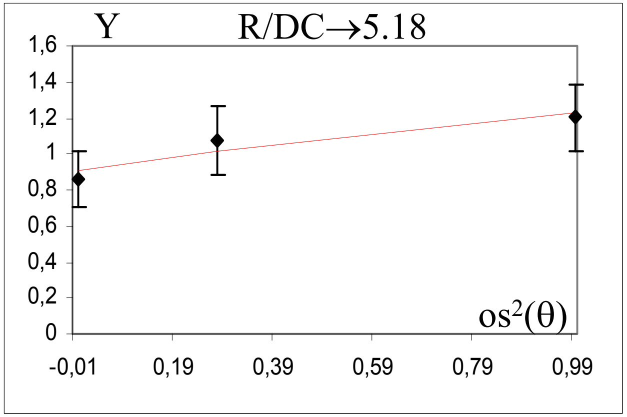

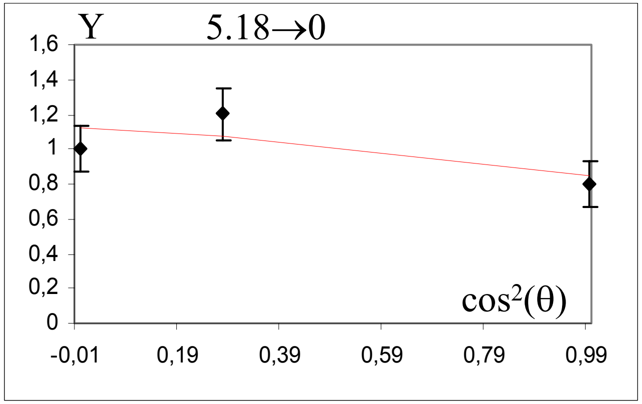

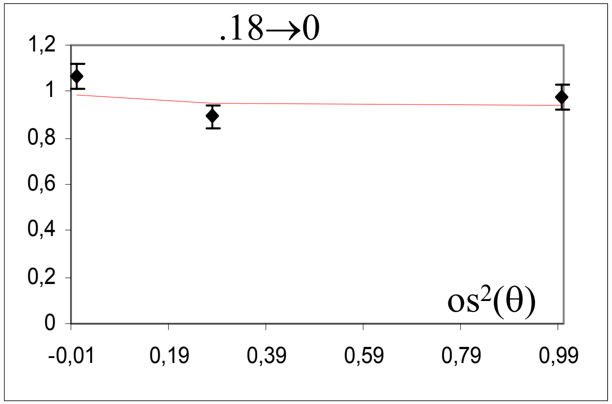

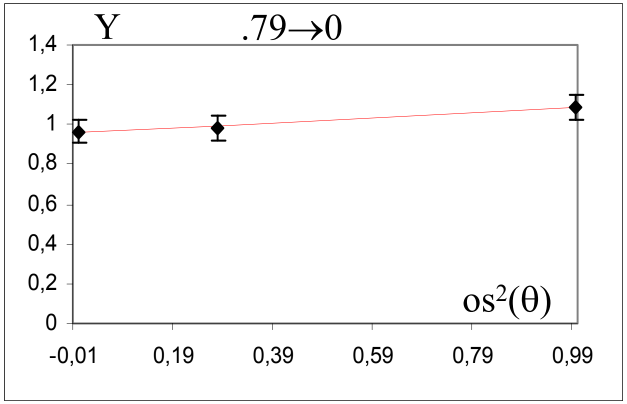

Data Analysis (1)

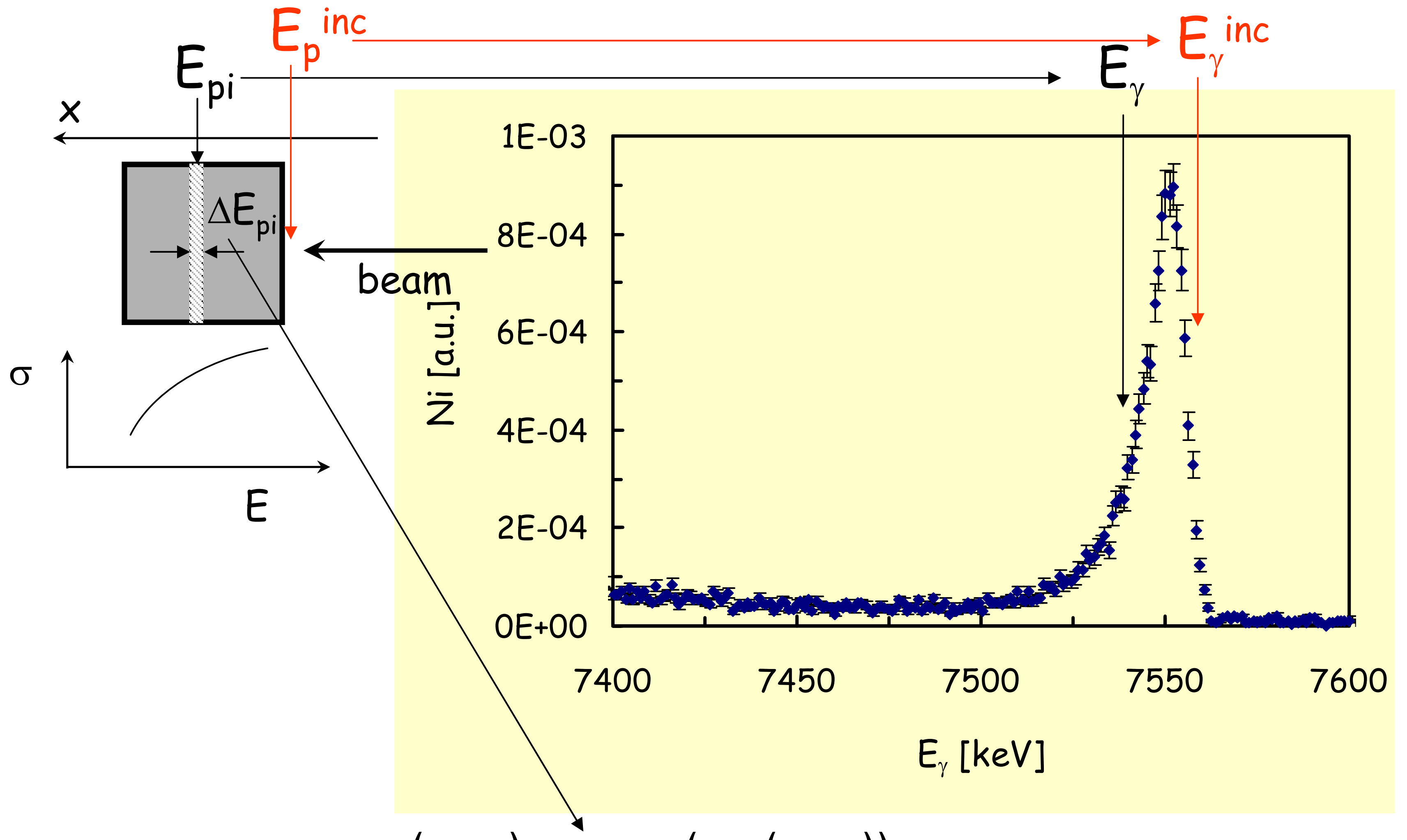

$$N_i = \frac{\sigma\left(E_{p_i}\right)\ \Delta E_\gamma \varepsilon\left(E_\gamma\left(E_{p_i}\right)\right)\ b_j}{\frac{dE}{dx}\left(E_{p_i}\right)}$$

Data Analysis (2)

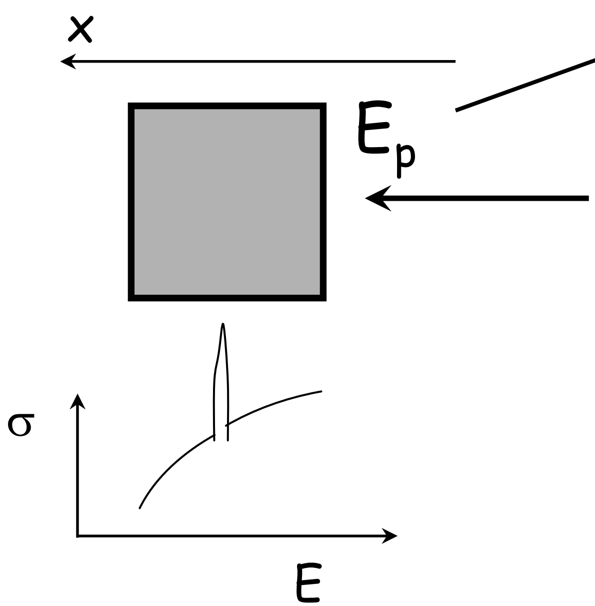

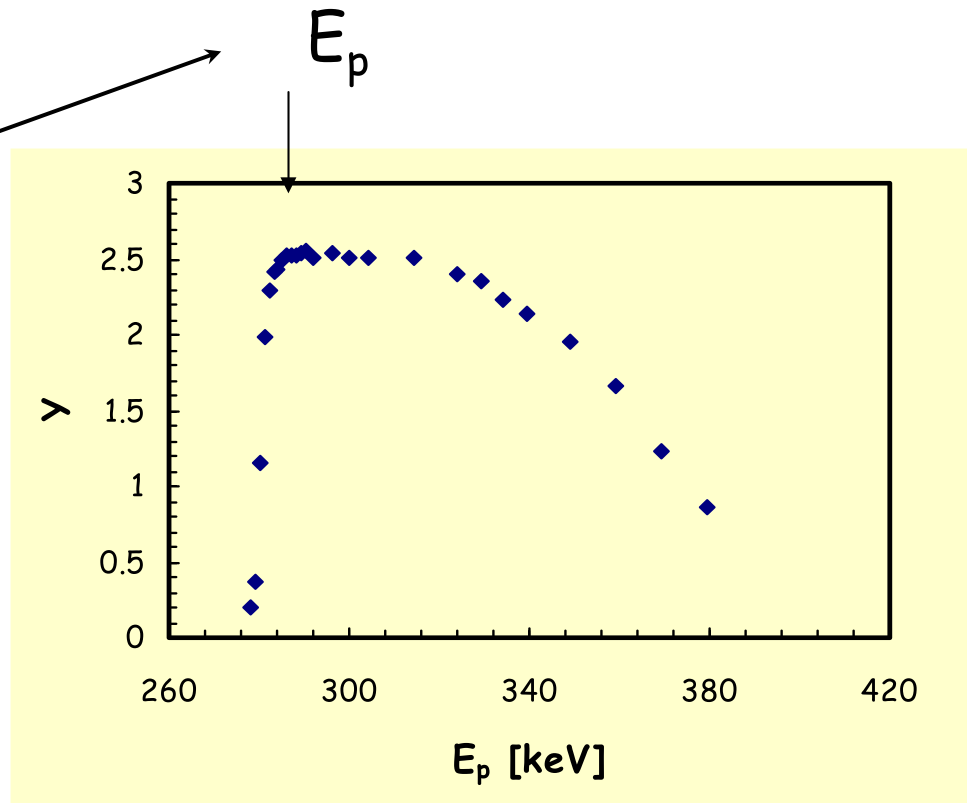

$$Y^{\infty} = \frac{\lambda^2}{2} \frac{\varpi\gamma b_j^R \varepsilon(E_\gamma^R)}{\frac{dE}{dx}(E_r)}$$

$$\frac{N_i}{Y^{\infty}} = \frac{2\sigma\left(E_{p_i}\right)\frac{dE}{dx}\left(E_{p_i}\right)\varepsilon\left(E_\gamma\right)\Delta E_\gamma b_j}{\lambda^2 \quad \varpi\gamma \frac{dE}{dx}\left(E_r\right)\varepsilon\left(E_\gamma^R\right)b_j^R}$$

Ground state results

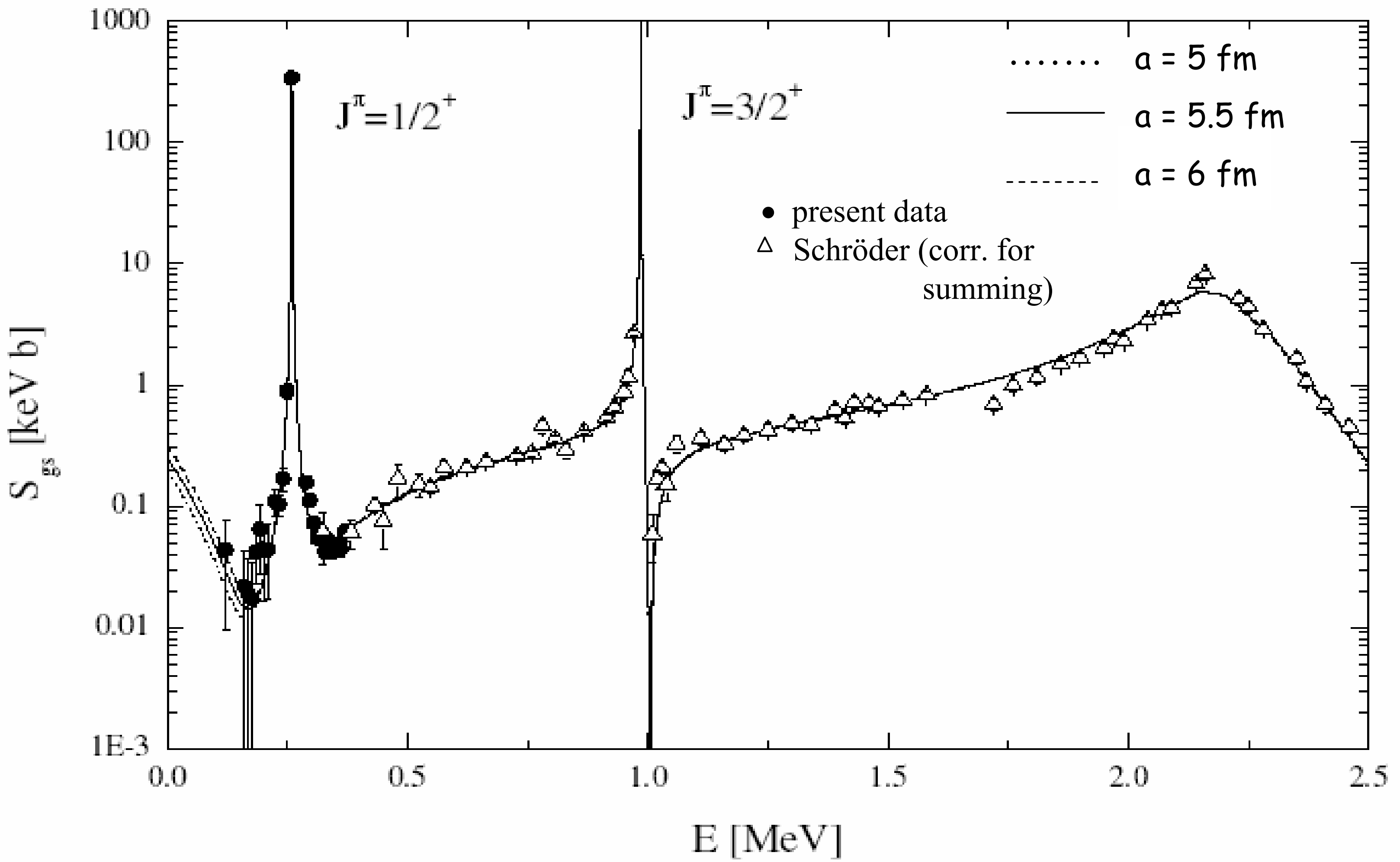

S_0^{gs} = 0.25 ± 0.06 keV b

R/DC→6.79 results

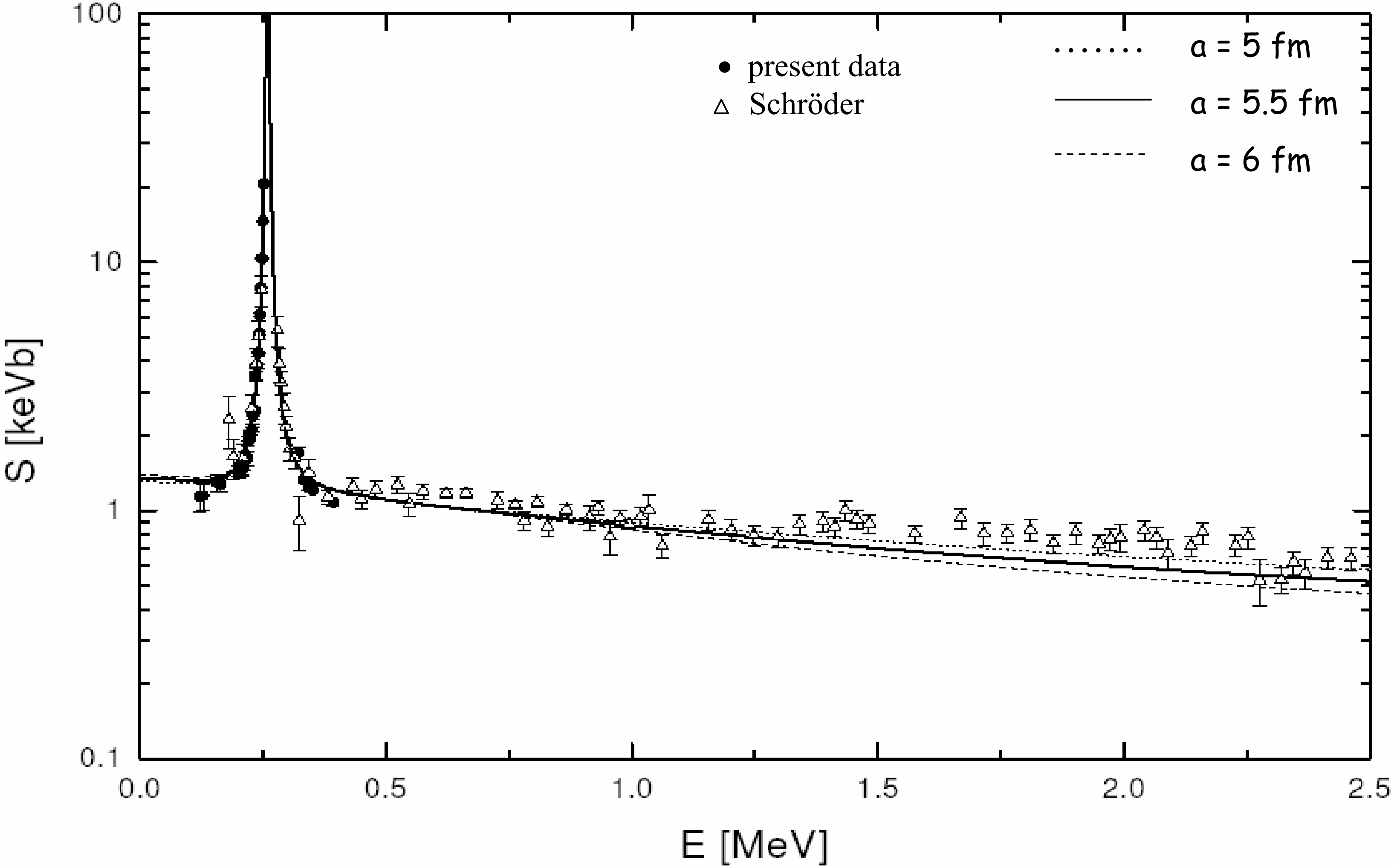

$S_0^{6.79} = 1.35 \pm 0.05$ keV b

Schröder('87) [*kev-b*]	Angulo ('01) [*kev-b*]
3.2 ± 0.5	1.8 ± 0.2

$$S_0^{tot} = 1.7 \pm 0.1 \text{ keV b}$$

Paper submitted to Phys. Letter B

- *GC age increases of 0.7-1 Gyr*
- CNO neutrino flux decreases a factor ≈ 2

Gas target set-up

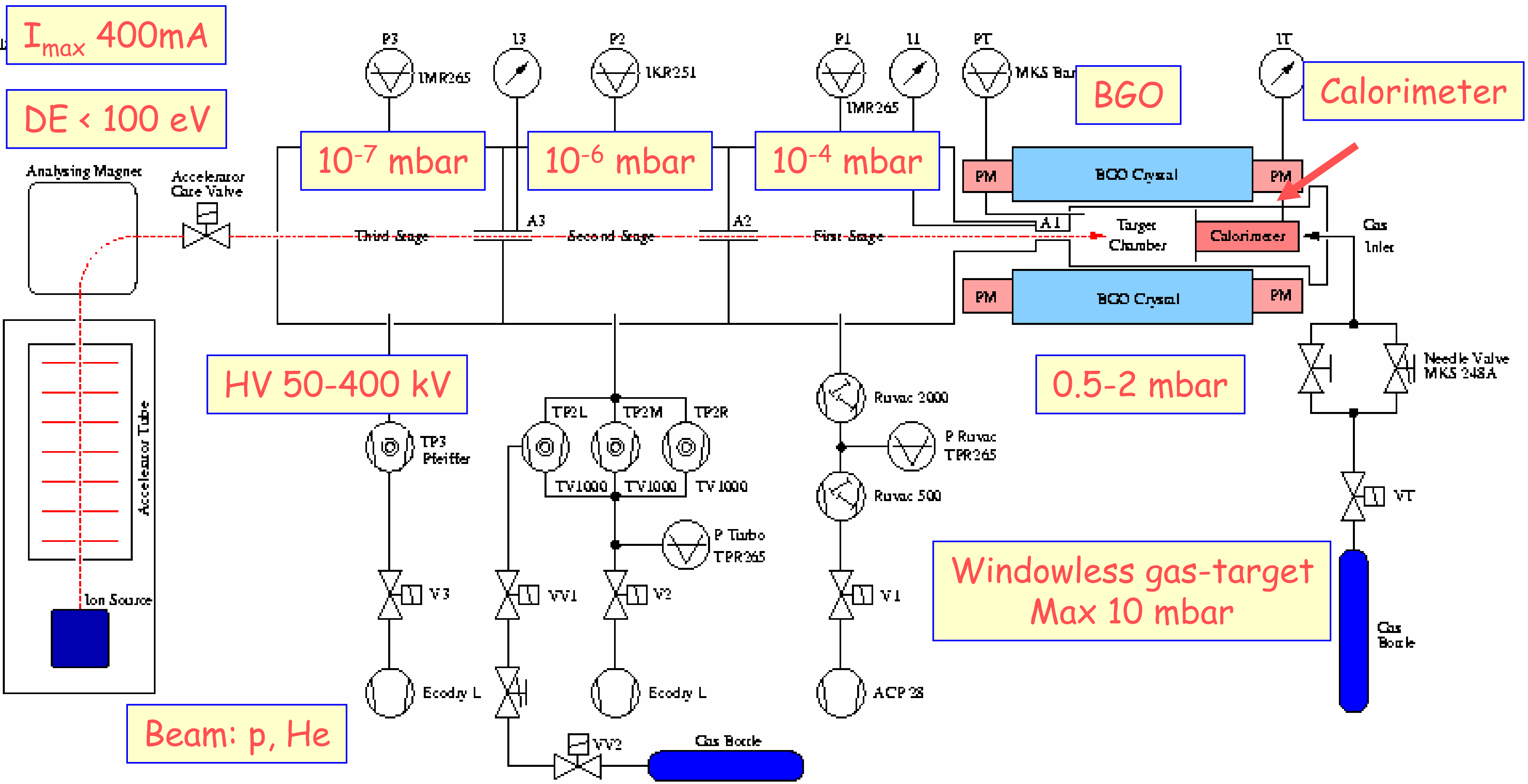

BGO detector

- Detection Efficiency ≈ 65 %
- Natural background (6500-8000 keV) → 20 c/day

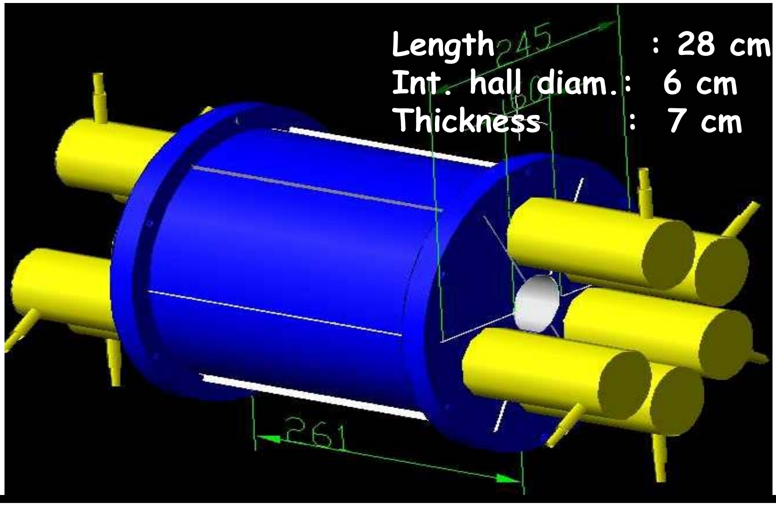

- Beam induced background

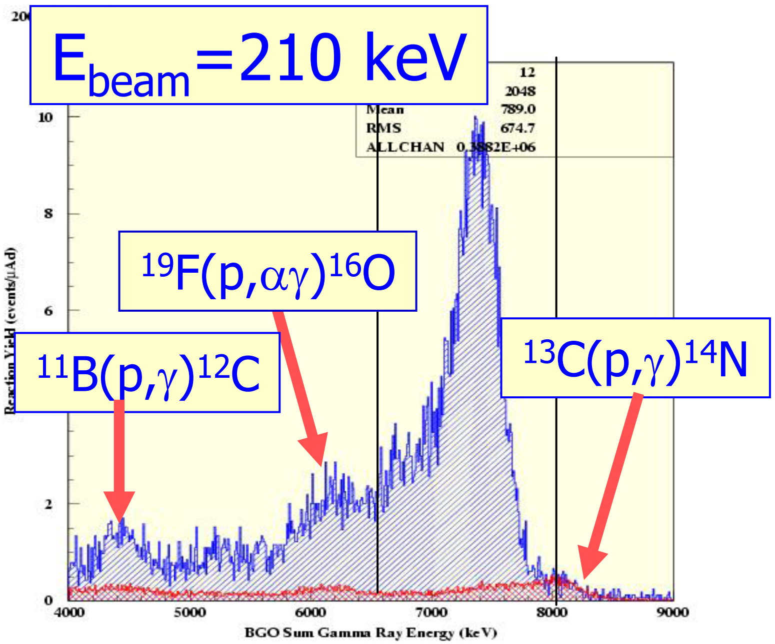

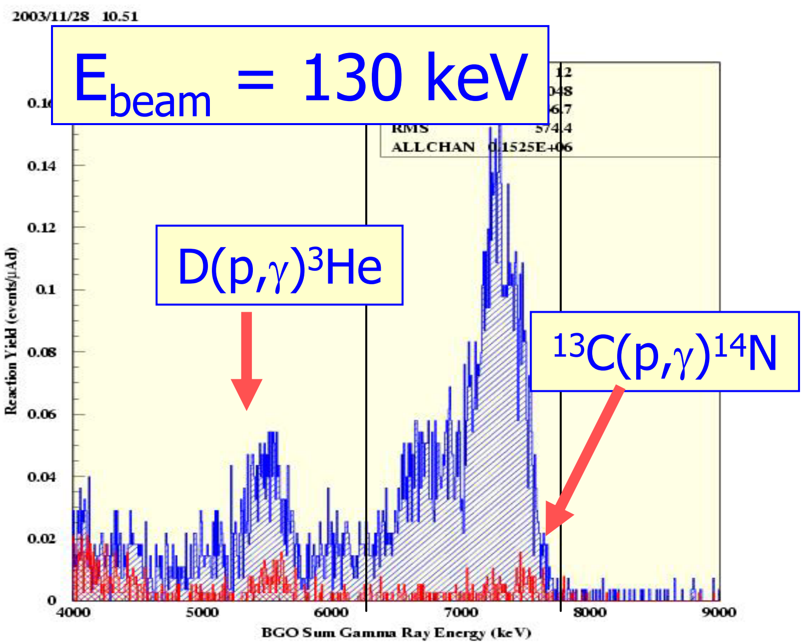

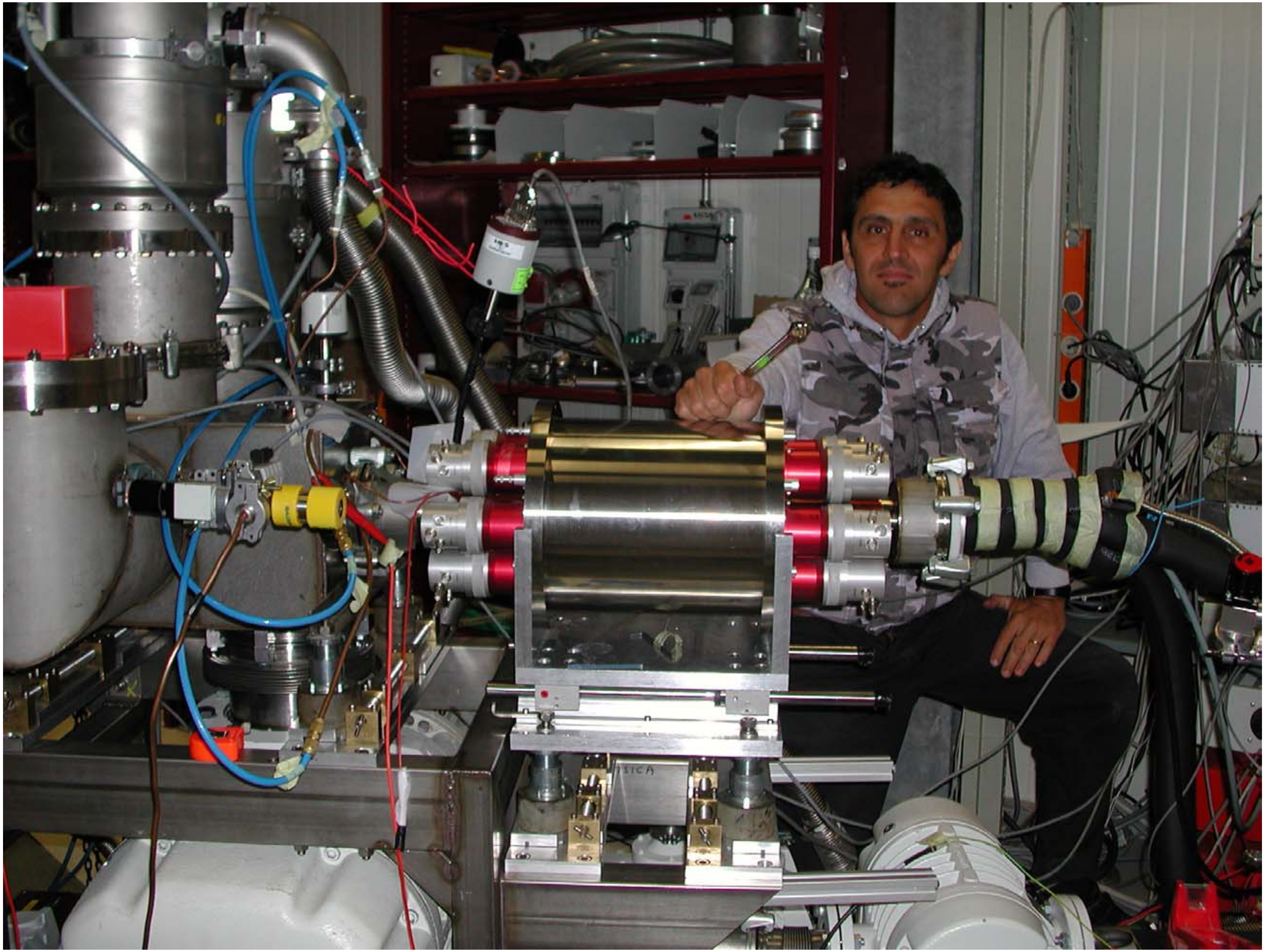

Data analysis(1)

Thin target

$$N_\gamma = N_{targ} N_{proj} \sigma(E_{cm})\, \eta\, \Delta z$$

Detector efficiency

Extended gas target

$$N_{targ}(z) = \nu \frac{P(z)}{kT}$$

$$E(z) = E_{beam} - \int_0^z \frac{dE}{dx} dz$$

$$N_\gamma = N_{proj} \frac{\nu}{kT} \int_0^L P(z)\, \sigma(E(z))\, \eta(z)\, dz$$

Data analysis(2)

Effective cross section

$$\sigma_{eff}\left(E_{effcm}\right)=\frac{N_\gamma}{N_{proj}\,\dfrac{\nu}{kT}\int_0^L P(z)\eta(z)\,dz}$$

Monte Carlo

$$N_{proj}=\frac{Q_{Beam}}{e}$$

$$E_{Eff}=E_{Beam}-\int_0^{z_{Eff}}\frac{dE}{d(\rho x)}\rho(z)\,dz$$

$$\int_0^L P(z)\eta(z)\,dz$$

Pressure profile along the target

Beam heating effect measurement

The particle beam heats the gas changing the local density.

Movable Lead Shielded NaI detector (1" x 1")

The 278 keV $^{14}N(p,\gamma)^{15}O$ resonance is positioned in front of the detector.

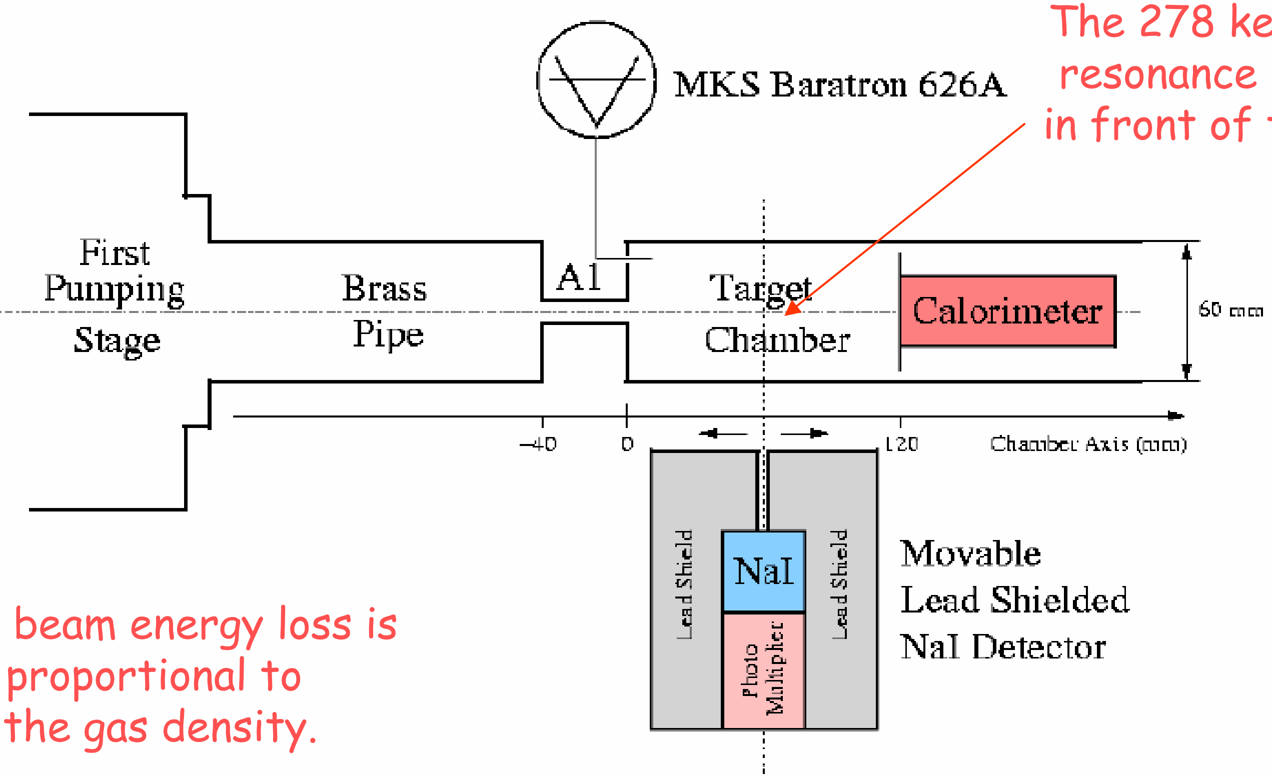

The beam energy loss is proportional to the gas density.

NaI detector

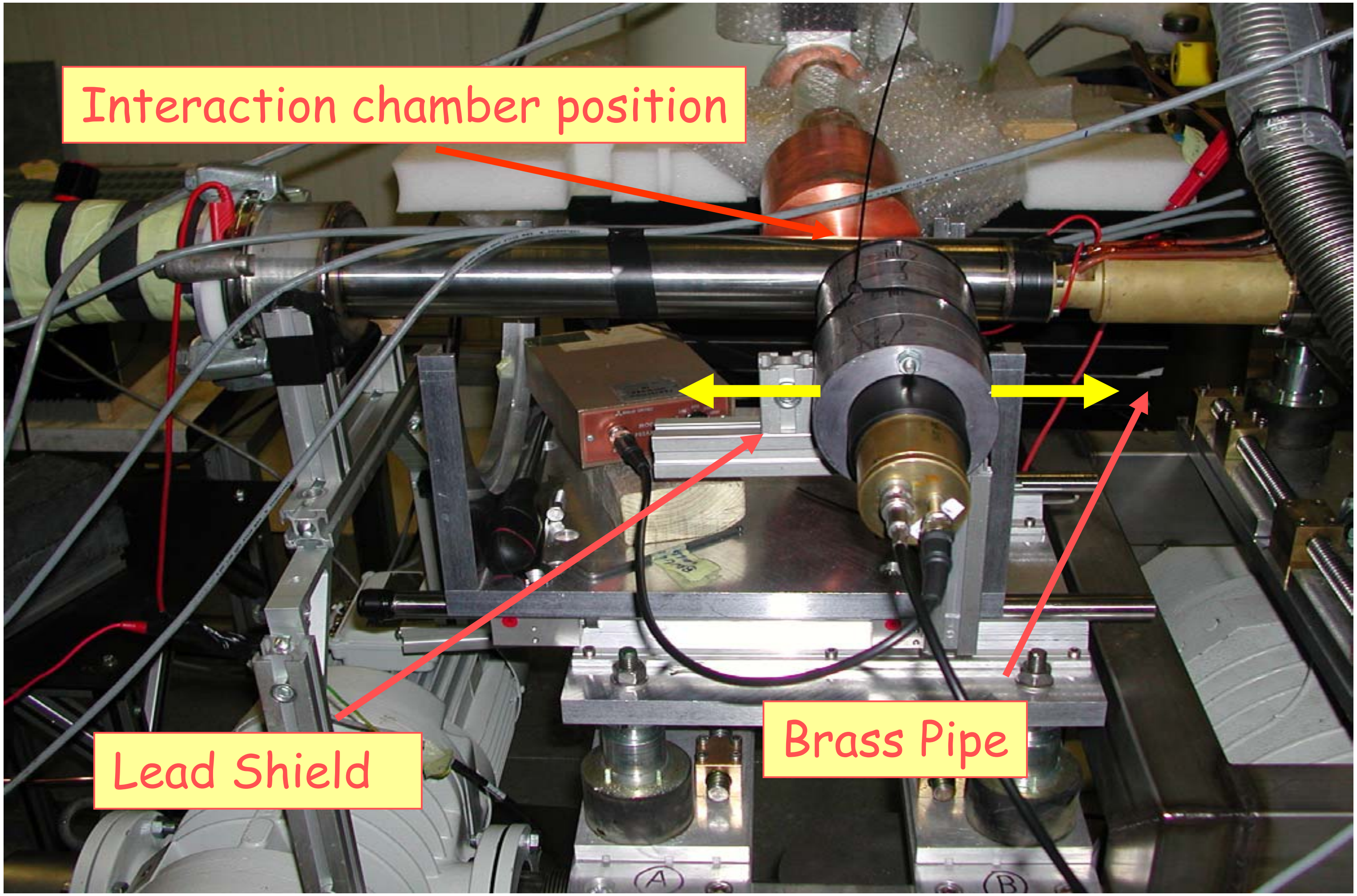

Pressure profile

$$\int_0^L P_t(z)\eta(z)\,dz$$

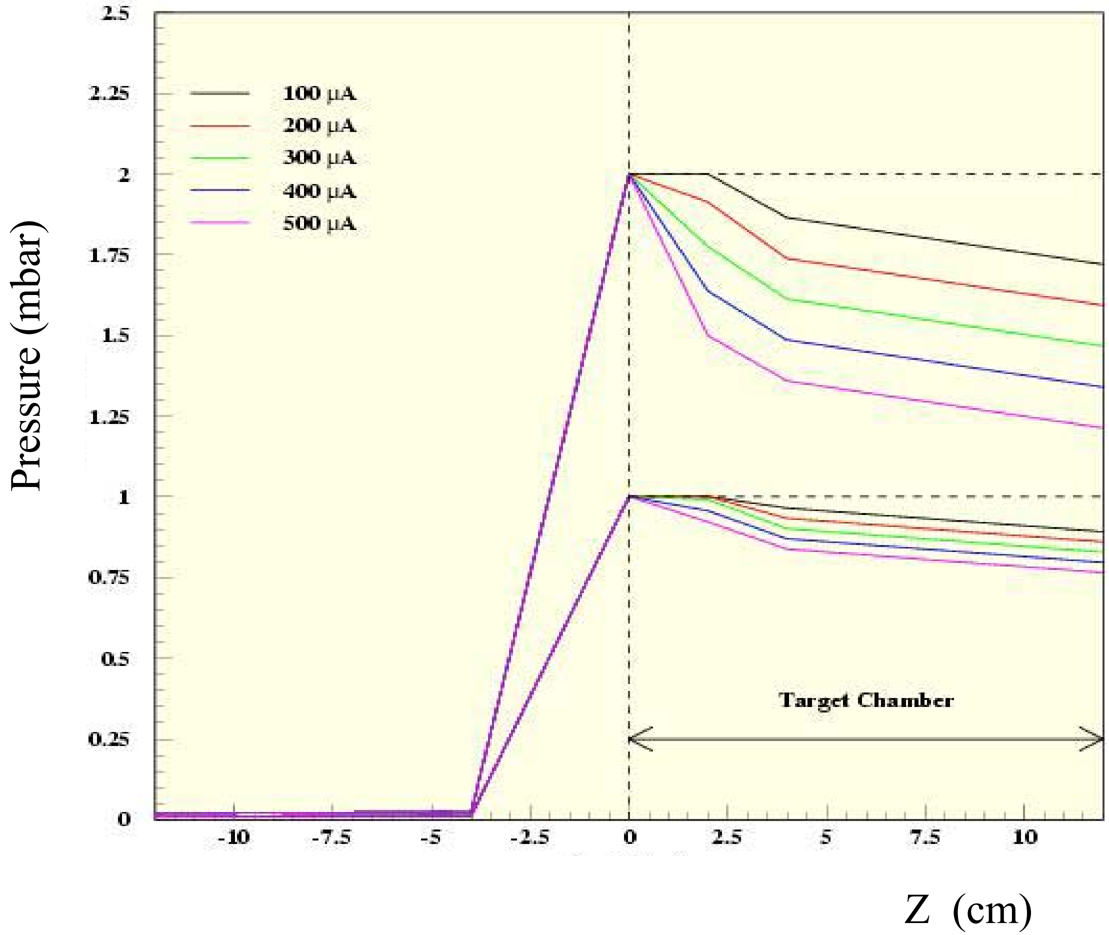

Cross Section preliminary data

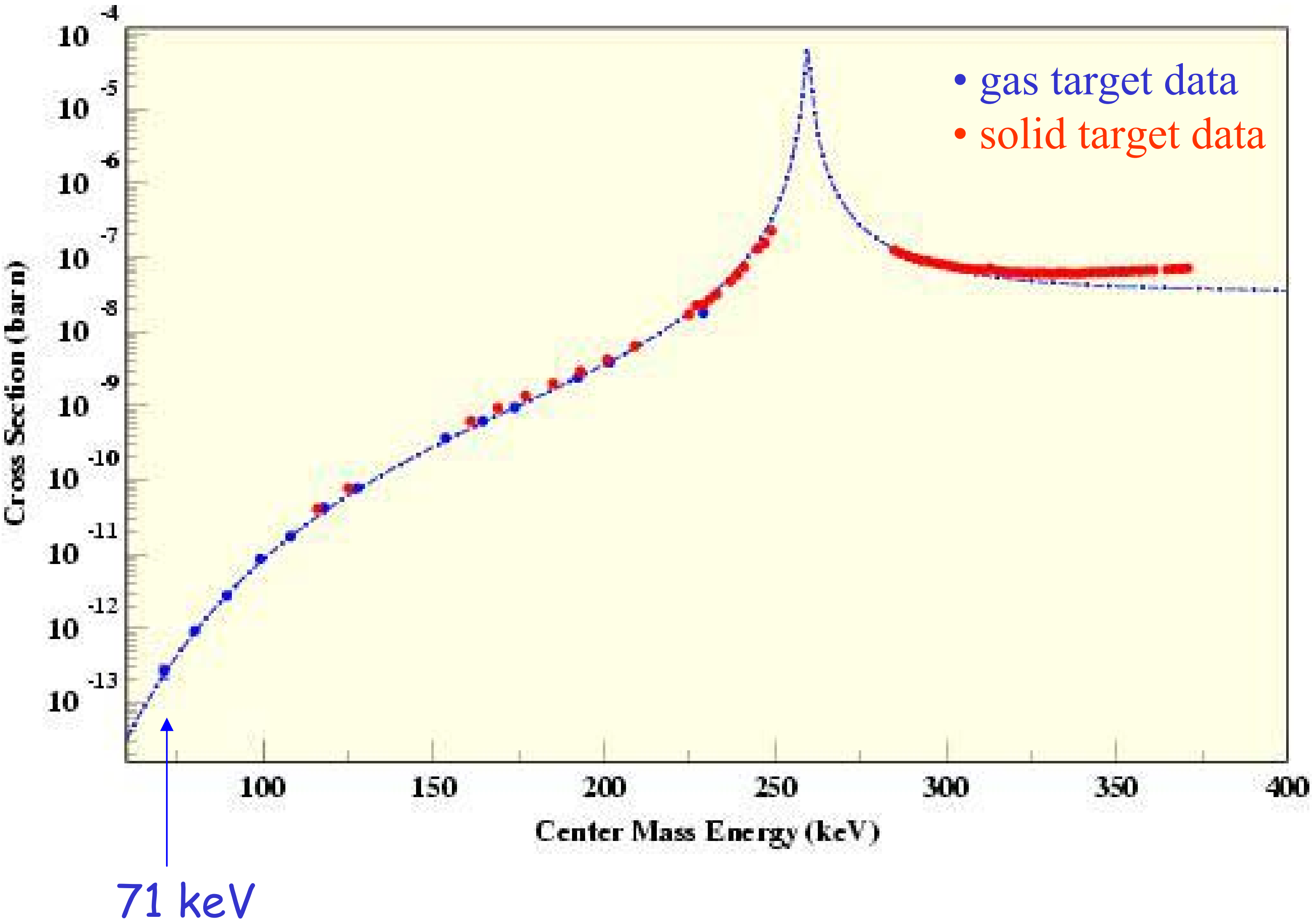

Ebeam = 80 keV

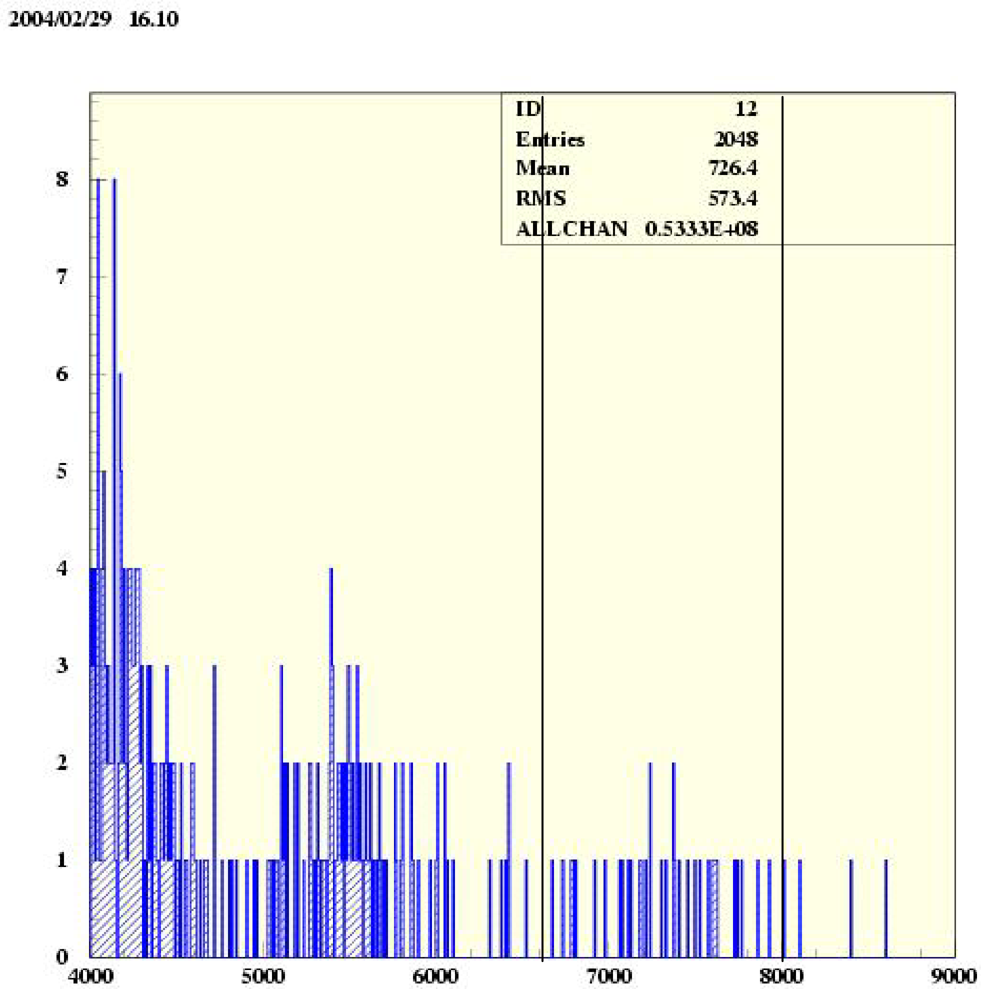
2004/02/29 16.10
ID 12
Entries 2048
Mean 726.4
RMS 573.4
ALLCHAN 0.5333E+08
0
1
2
3
4
5
6
7
8
4000
5000
6000
7000
8000
9000

ωγ measurement(1)

BGO Resonance Scan at 2 mbar (77 μA)

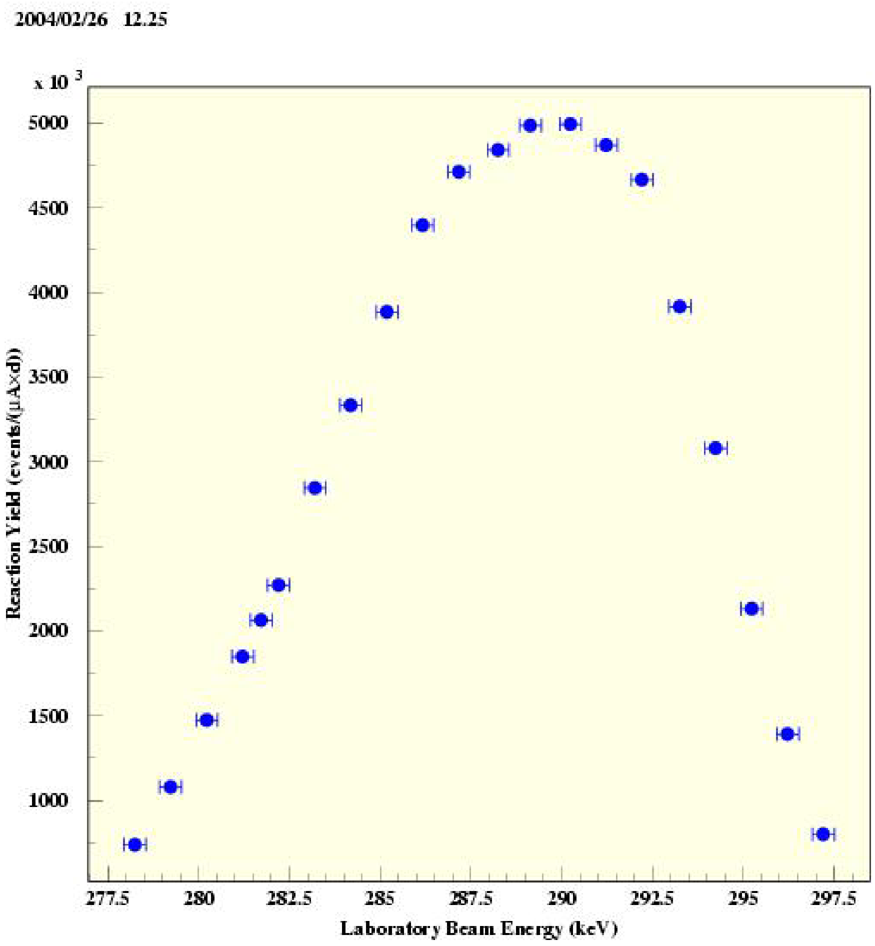

Pressure	ωγ (meV)
2.0 mbar	13.6 ± 0.8

Solid Target: 13.5 ± 0.4 ± 0.8

Other Works 14 ± 1

$\omega\gamma$ measurement(1)

BGO Resonance Scan at 2 mbar (77 μA)

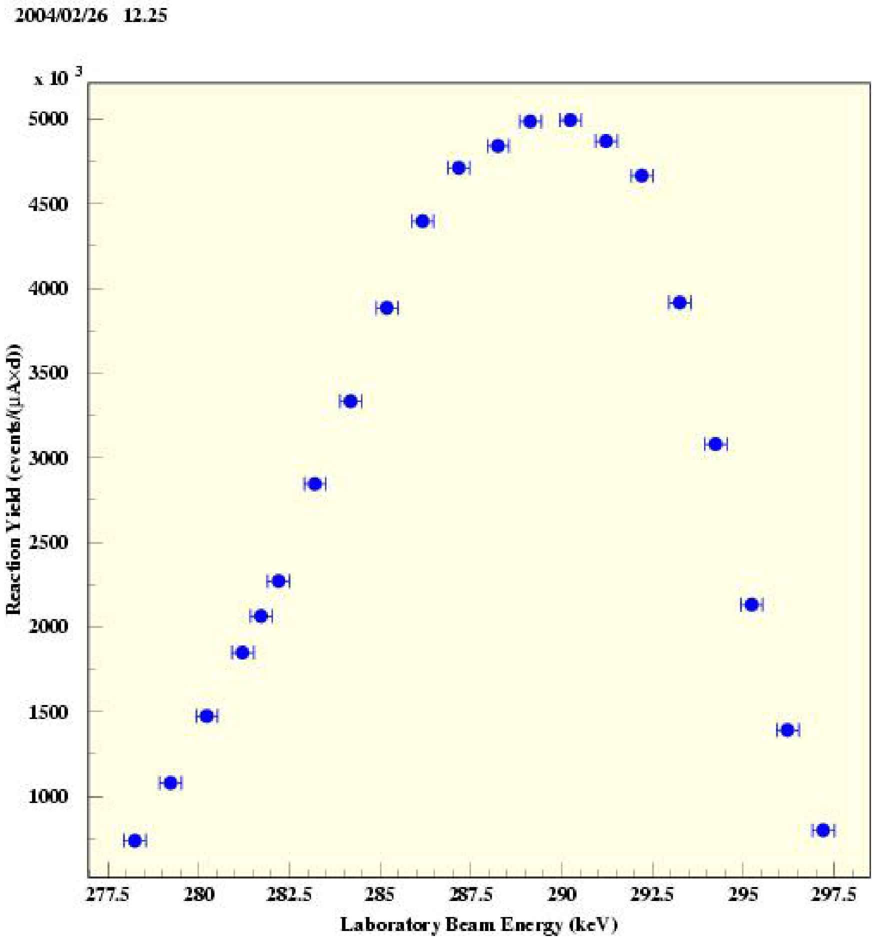

Pressure	$\omega\gamma$ (meV)
2.0 mbar	13.6 ± 0.8
1.0 mbar	12.7 ± 0.7
0.5 mbar	11.3 ± 0.6

Solid Target: $13.5 \pm 0.4 \pm 0.8$

Other Works 14 ± 1

ωγ measurement(2)

Assuming η and ρ as constants

$$Y(E_b,\rho)=\frac{N_d}{Q}=\int_0^L \sigma(E(z))\rho(z)\eta(z)dz \approx \frac{\bar{\eta}}{\frac{dE}{d(\rho x)}}\int_{E_b}^{E_b-\Delta}\sigma(E)dE$$

Because Amplitude energy dependence is negligible:

$$\int_0^\infty \sigma_{bw}(E)dE=\frac{\lambda^2}{2}\omega\gamma$$

<u>IF</u> $\Delta > 6\Gamma$

$$\omega\gamma=\frac{Y_{\max}}{\frac{\lambda^2}{2}\frac{M+m}{M}\frac{\bar{\eta}}{\frac{dE}{d(\rho x)}}}$$

ωγ measurement(3)

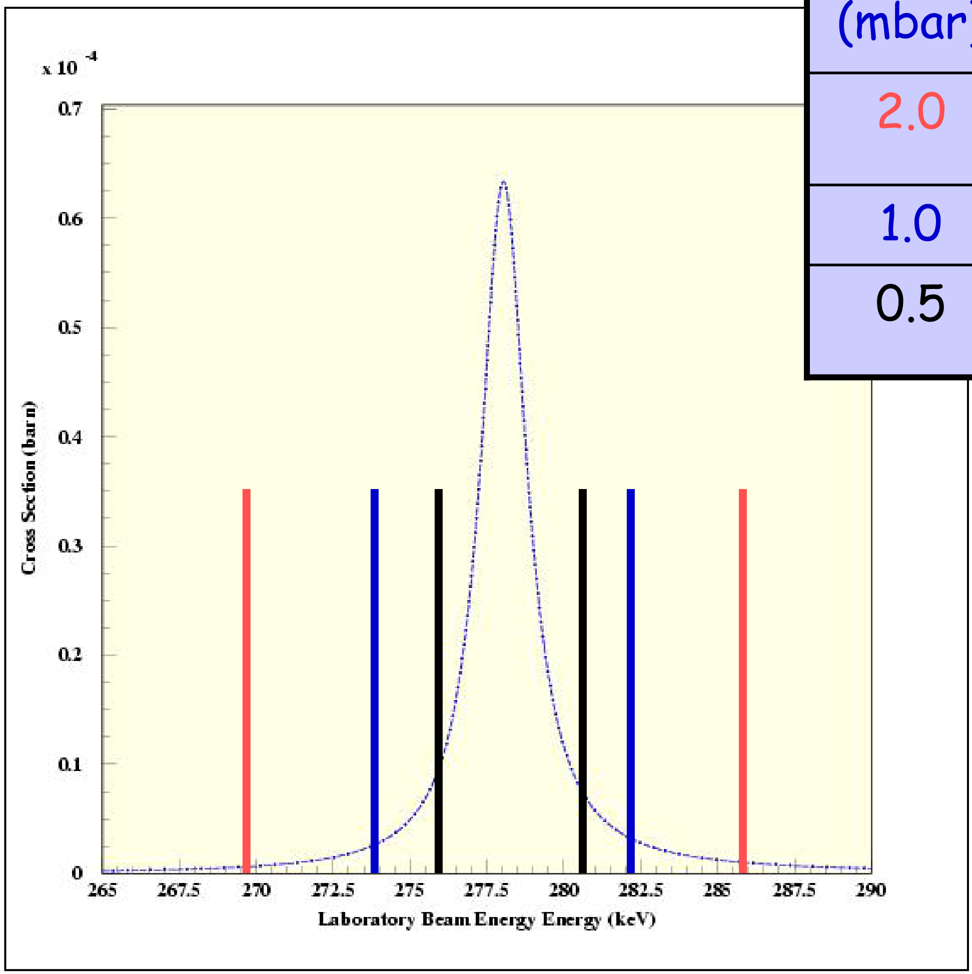

P (mbar)	Δ	% $\sigma_{BW}(E)$ integral	Experimental ratio
2.0	9.3 Γ	≅ 100	1
1.0	4.9 Γ	93	.93 + .08
0.5	2.4 Γ	81	.83 + .07

No appreciable systematic effects but...

Further scans at 1.5 and 3 mbar

Future perspectives(1) $^{4}He(^{3}He,\gamma)^{7}Be$

- Φ_B depends on nuclear physics and astrophysics inputs
- $\Phi_B = \Phi_B^{(SSM)} \cdot s_{33}^{-0.43} s_{34}^{0.84} s_{17}^{1} s_{e7}^{-1} s_{pp}^{-2.7} \cdot com^{1.4} opa^{2.6} dif^{0.34} lum^{7.2}$
- These give flux variation with respect to the SSM calculation when the input X is changed by $x = X/X^{(SSM)}$.
- Can learn astrophysics if nuclear physics is known well enough.

•Nuclear physics uncertainties, particularly on S_{34}, dominate over the present observational accuracy $\Delta\Phi_B/\Phi_B = 7\%$.

•The foreseeable accuracy $\Delta\Phi_B/\Phi_B = 3\%$ could illuminate about solar physics if a significant improvement on S_{34} is obtained

Source	ΔX/X (1σ)	$\Delta\Phi_B/\Phi_B$ (1σ)
S33	0.06	0.03
S34	0.09	0.08
S17	0.05 ?	0.05
Se7	0.02	0.02
Spp	0.02	0.05
Com	0.06	0.08
Opa	0.02	0.05
Dif	0.10	0.03
Lum	0.004	0.03

$^4He(^3He,\gamma)^7Be$

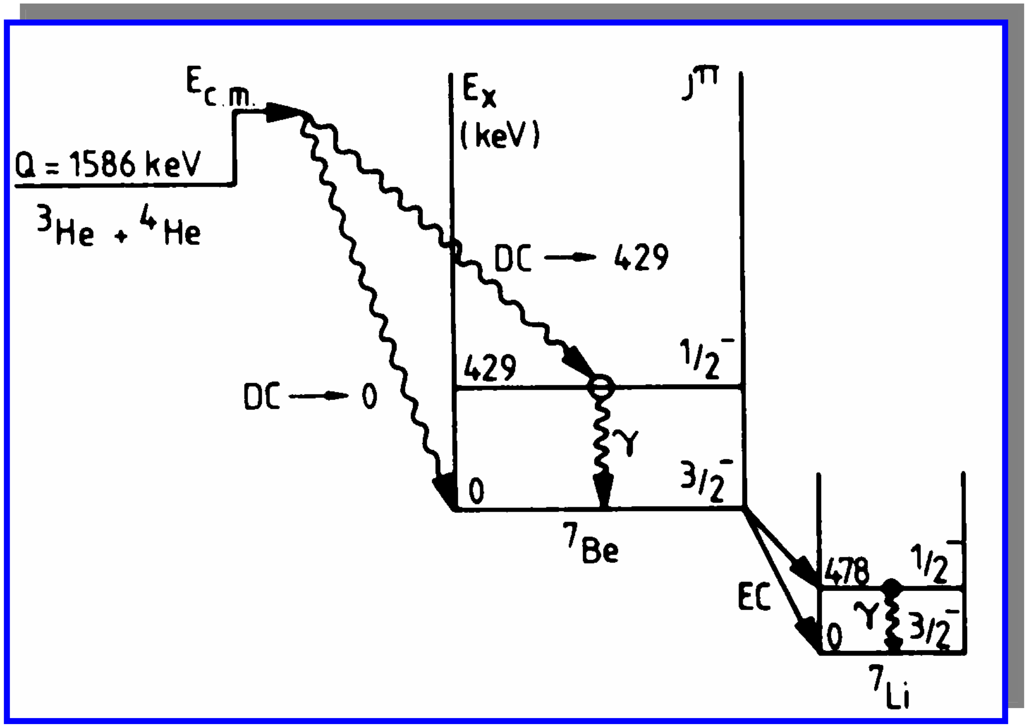

Mainly 3 γ-transitions:

- ✓ $E\gamma$ =1585 keV + E_{cm} (DC→0);
- ✓ $E\gamma$ = 1157 keV + E_{cm} and $E\gamma$ = 429 keV (DC→0.429; 0.429 →0)

Past measurements

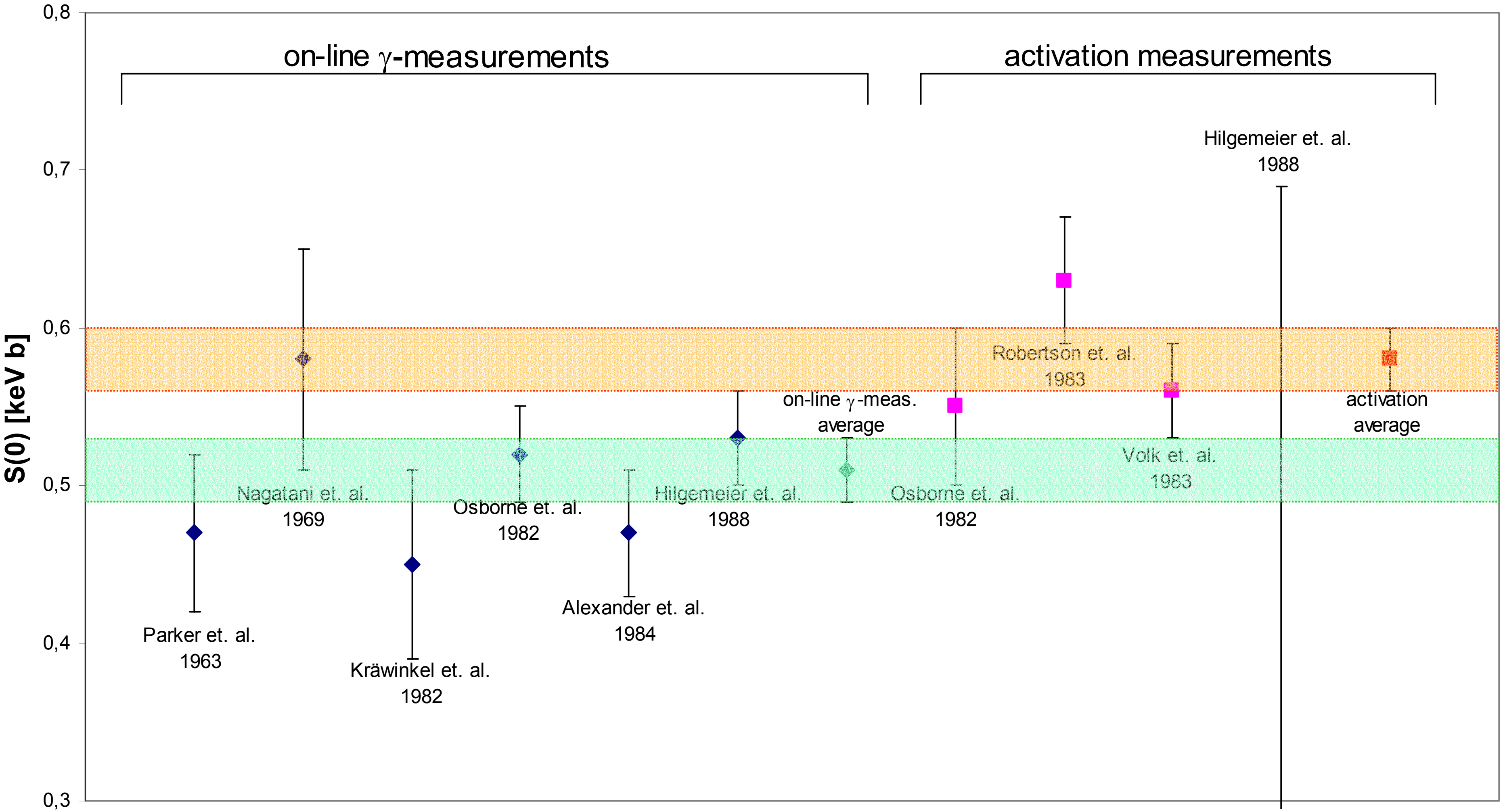

Target chamber design (1)

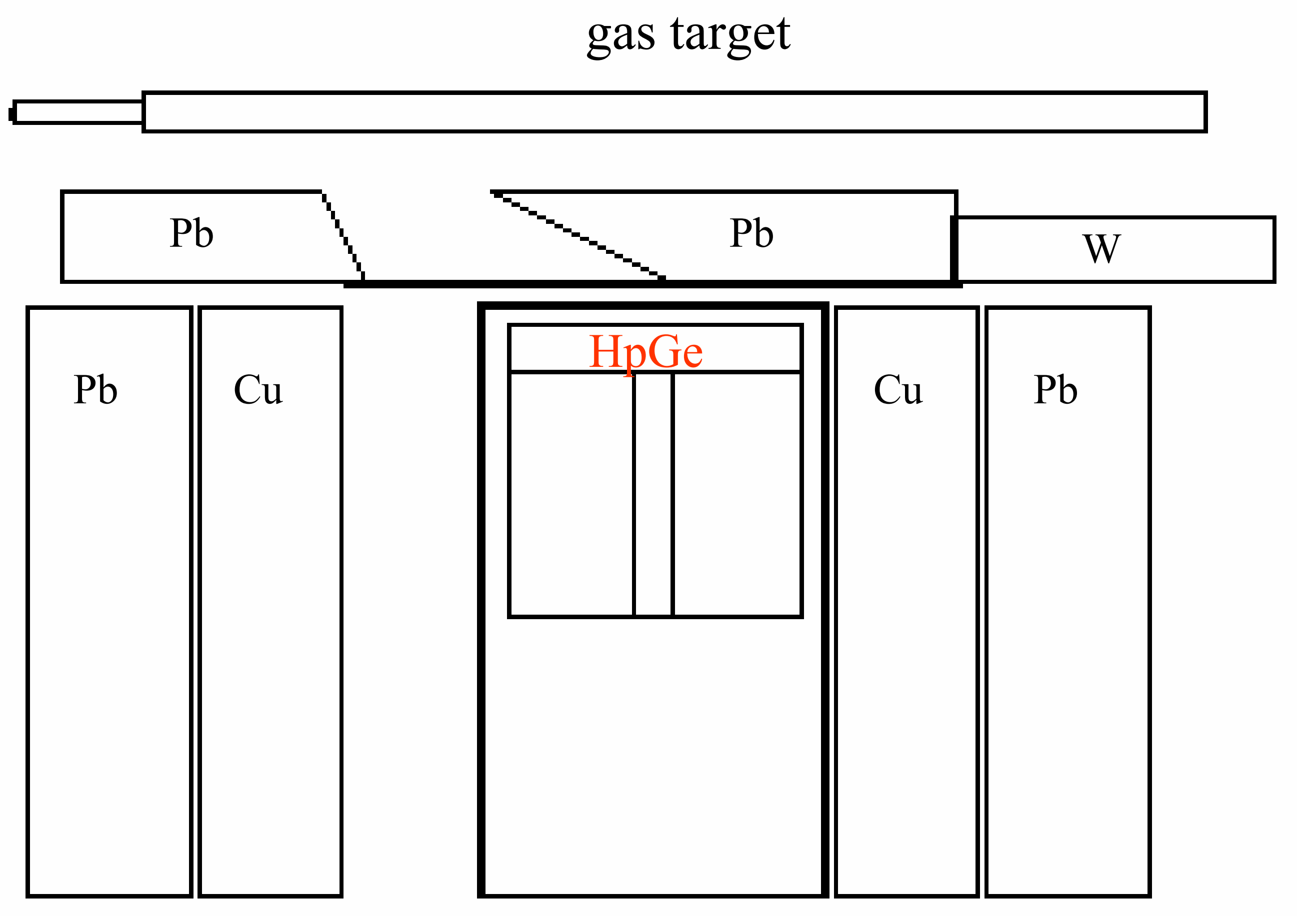

Target chamber design

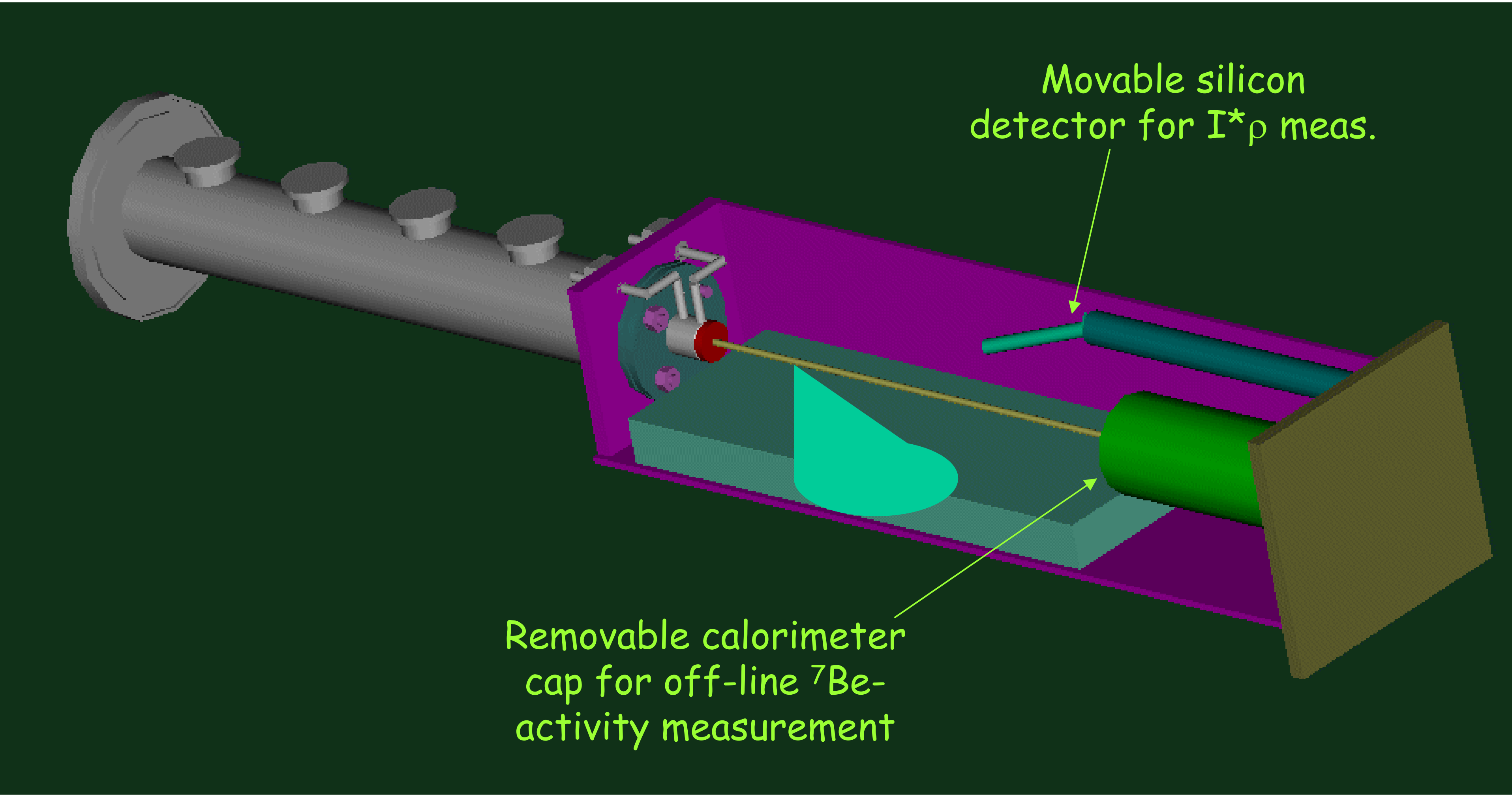

Expected counting rate

P = 1 mbar; I = 200 μA

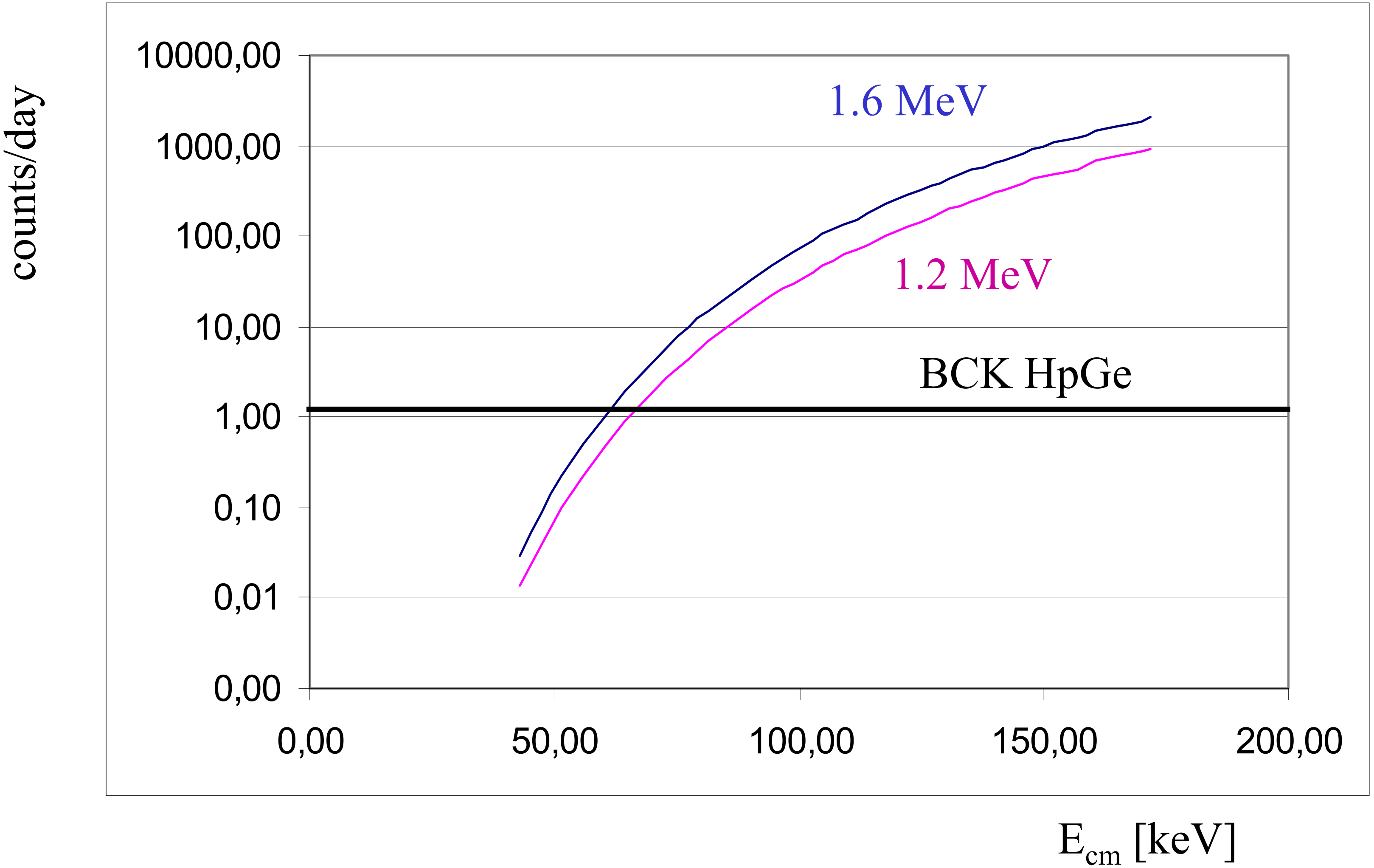

Future perspectives(2) $^{25}Mg(p,\gamma)^{26}Al$

$^{25}Mg(p,\gamma)$ is the main production mechanism for ^{26}Al in astrophysical scenarios

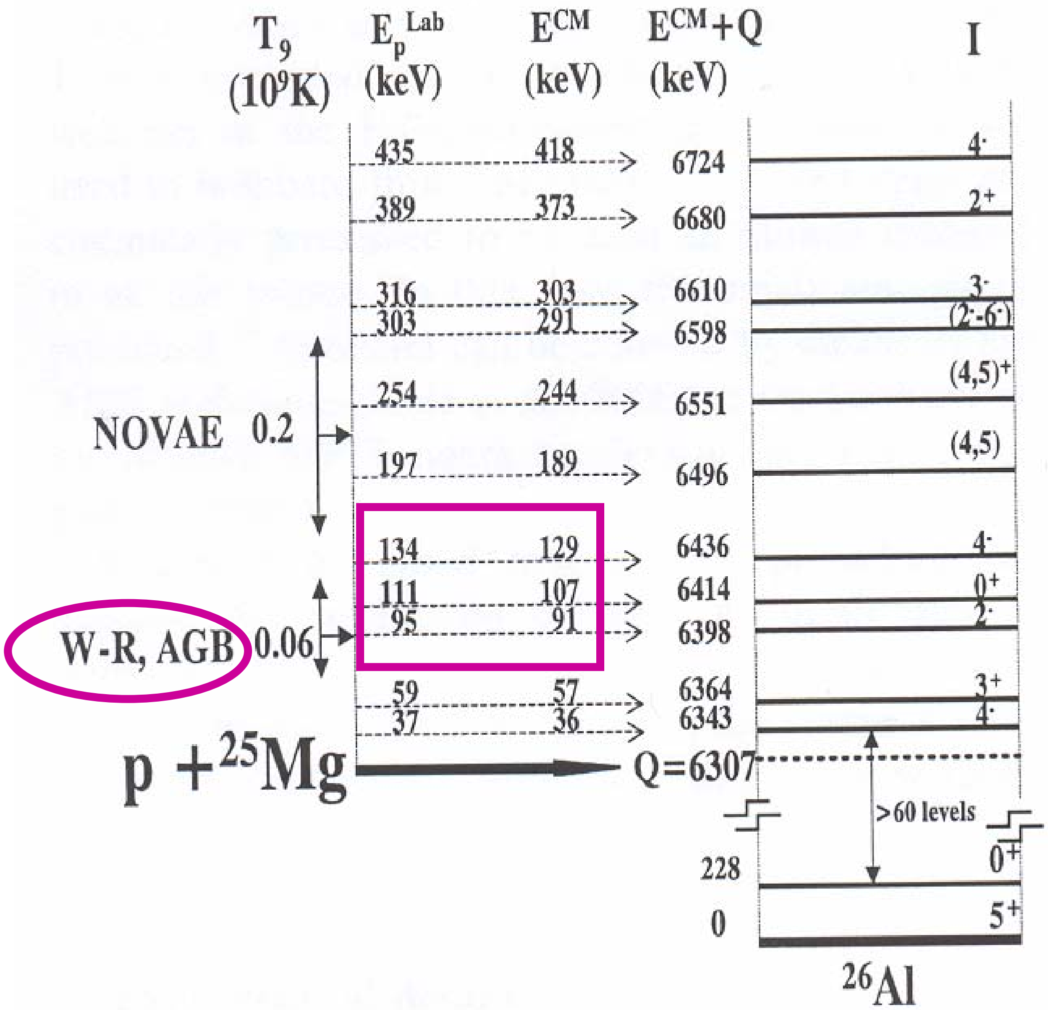

E_p^{lab}(keV)	$\omega\gamma$ (eV)
135.1	$<1.4 \times 10^{-10}$
112.2	$(3\pm1) \times 10^{-11}$
95.8	$(1\pm0.3) \times 10^{-10}$
59.7	$(3\pm1) \times 10^{-13}$
38.4	$<2.4 \times 10^{-20}$

E_γ= 6436 keV

E_γ= 6398 keV

Resonance strengths calculated from the $^{25}Mg(^{3}He,d)^{26}Al$ reaction (Iliadis et al 1996)

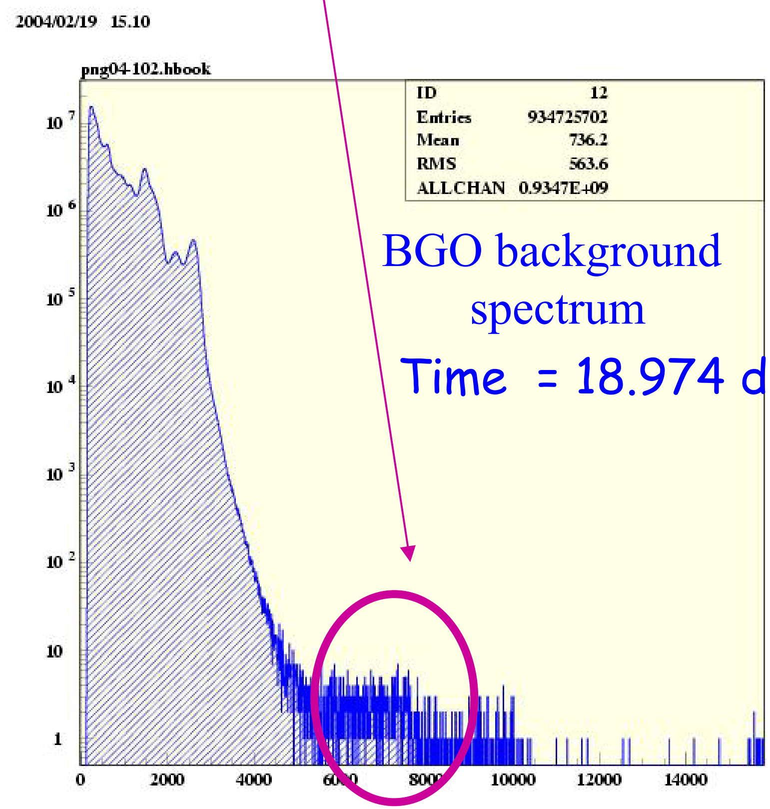

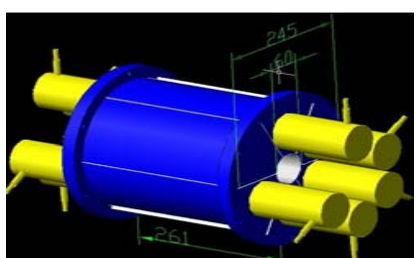

Conclusions

- $^{14}N(p,\gamma)^{15}O$ has been studied with a solid target set-up down to E_{cm}=135 keV

- Present work improves the experimental information concerning the R/DC→0 transition

- Using a gas target set-up the $^{14}N(p,\gamma)^{15}O$ total cross-section is presently studied at LUNA down to E_{cm}=70 keV

- Future measurements are :

  $^{4}He(^{3}He,\gamma)^{7}Be$ (gas target)

  $^{25}Mg(p,\gamma)^{26}Al$ (solid target)